International Ocean Discovery Program Expedition 390C Preliminary Report

South Atlantic Transect Reentry Systems

5 October–5 December 2020

Emily R. Estes, Trevor Williams, Stephen Midgley, Rosalind M. Coggon, Jason B. Sylvan, Gail L. Christeson, and Damon A.H. Teagle

IODP
INTERNATIONAL OCEAN DISCOVERY PROGRAM

Publisher's notes

Core samples and the wider set of data from the science program covered in this report are under moratorium and accessible only to Science Party members until 7 February 2024.

This publication was prepared by the *JOIDES Resolution* Science Operator (JRSO) at Texas A&M University (TAMU) as an account of work performed under the International Ocean Discovery Program (IODP). Funding for IODP is provided by the following international partners:

National Science Foundation (NSF), United States
Ministry of Education, Culture, Sports, Science and Technology (MEXT), Japan
European Consortium for Ocean Research Drilling (ECORD)
Ministry of Science and Technology (MOST), People's Republic of China
Korea Institute of Geoscience and Mineral Resources (KIGAM)
Australia-New Zealand IODP Consortium (ANZIC)
Ministry of Earth Sciences (MoES), India
Coordination for Improvement of Higher Education Personnel (CAPES), Brazil

Portions of this work may have been published in whole or in part in other IODP documents or publications.

Disclaimer

Copyright

Citation

Emily R. Estes, Trevor Williams, Stephen Midgley, Rosalind M. Coggon, Jason B. Sylvan, Gail L. Christeson, and Damon A.H. Teagle, 2021. *Expedition 390C Preliminary Report: South Atlantic Transect Reentry Systems*. International Ocean Discovery Program. https://doi.org/10.14379/iodp.pr.390C.2021

ISSN

World Wide Web: 2372-9562

April 2021

Expedition 390C participants

Expedition 390C scientists

Emily R. Estes
Expedition Project Manager/Staff Scientist Expedition 390/390C (shipboard)
International Ocean Discovery Program
Texas A&M University
USA
estes@iodp.tamu.edu

Trevor Williams
Expedition Project Manager/Staff Scientist Expedition 393/395E (shore based)
International Ocean Discovery Program
Texas A&M University
USA
williams@iodp.tamu.edu

Rosalind M. Coggon
Co-Chief Scientist Expedition 390 (shore based)
School of Ocean and Earth Science
University of Southampton
United Kingdom
R.M.Coggon@soton.ac.uk

Jason B. Sylvan
Co-Chief Scientist Expedition 390 (shore based)
Department of Oceanography
Texas A&M University
USA
jasonsylvan@tamu.edu

Gail L. Christeson
Co-Chief Scientist Expedition 393 (shore based)
Institute for Geophysics
University of Texas at Austin
USA
gail@ig.utexas.edu

Damon A.H. Teagle
Co-Chief Scientist Expedition 393 (shore based)
School of Ocean and Earth Science
University of Southampton
United Kingdom
Damon.Teagle@southampton.ac.uk

Operational and technical staff

Siem Offshore AS officials

Harm Cornelis Theodoor Nienhuis
Master of the Drilling Vessel

Curtis Wayne Lambert Jr
Drilling Supervisor

JRSO shipboard personnel and technical representatives

Alexis Armstrong
Core Laboratory

Heather Barnes
Assistant Laboratory Officer

James Brattin
Applications Developer

Michael Cannon
Marine Computer Specialist

Etienne Claassen
Marine Instrumentation Specialist

Clayton Furman
Logging Engineer (Schlumberger)

Luan Heywood
Thin Section Laboratory

Sarah Kachovich
Imaging Specialist

Jurie Kotze
Marine Instrumentation Specialist

Brittany Martinez
Curatorial Specialist

Stephen Midgley
Operations Superintendent

Eric Moortgat
Assistant Laboratory Officer

Kerry Mullins
Marine Computer Specialist

Jenna Patten
X-Ray Laboratory

Chieh Peng
Laboratory Officer

Vincent Percuoco
Chemistry Laboratory

Doris Piñero Lajas
Physical Properties Laboratory

Alexander Roth
Paleomagnetism Laboratory

Johanna Suhonen
Chemistry Laboratory

Abstract

International Ocean Discovery Program (IODP) Expedition 390C was implemented in response to the global COVID-19 pandemic and occupied sites proposed for the postponed Expeditions 390 and 393. The objectives for Expedition 390C were to core one hole at each site with the advanced piston corer/extended core barrel (APC/XCB) system to basement for gas safety monitoring and to install a reentry system with casing through the sediment to between ~5 m above basement and <5 m into basement in a second hole. These operations will expedite basement drilling during the rescheduled South Atlantic Transect Expeditions 390 and 393. The six primary sites for those expeditions form a transect perpendicular to the Mid-Atlantic Ridge on the South American plate, overlying crust ranging in age from 7 to 61 Ma. Basement coring will increase our understanding of how crustal alteration progresses over time across the flanks of a slow/intermediate spreading ridge and how microorganisms survive in deep subsurface environments. Sediment will be used in paleoceanographic and microbiological studies. Expedition 390C started in Kristiansand, Norway, and ended in Cape Town, South Africa, after 31 days of operations. We cored a single APC/XCB sediment hole to the contact with hard rock material at four of the six sites and successfully installed reentry systems with casing at three. Two failed attempts at drilling in casing and a reentry system into hard rock at Site U1558 indicate that the Dril-Quip reentry cones and running tools are incompatible with use in hard rock because the release mechanism does not work when the casing string weight cannot be fully removed from the running tool. Therefore, at Sites U1558 and U1559, casing was installed to ~10 m above basement. Site U1557 has a thick sediment cover (564 m) and will require multiple casing strings to reach basement; a single 16" casing string was installed to 60 meters below seafloor at this site, and later expeditions will extend casing.

Introduction

Expedition 390C was conceived in response to the global COVID-19 pandemic that resulted in the postponement of multiple International Ocean Discovery Program (IODP) expeditions in 2020 and 2021. With science parties unable to travel to the vessel, we were nonetheless able to utilize vessel time by sending a small team of IODP staff to complete engineering work in advance of IODP South Atlantic Transect (SAT) Expeditions 390 and 393. The objectives for Expedition 390C were to core one hole at each site with the advanced piston corer/extended core barrel (APC/XCB) system to basement for gas safety monitoring and to install a reentry system with casing through the sediment to between ~5 m above basement and <5 m into basement in a second hole. Having reentry systems in place at each site decreases the operational risk of the SAT expeditions and better guarantees we recover the material needed to achieve the science objectives. The APC/XCB cores recovered during Expedition 390C will be considered part of Expeditions 390 and 393.

Expeditions 390 and 393 will recover complete sedimentary sections and the upper ~250 m of underlying ocean crust at six sites along a slow/intermediate spreading rate Mid-Atlantic Ridge (MAR) crustal flow line at ~31°S (Figure **F1**). The expeditions will operate in a region last visited during Deep Sea Drilling Project (DSDP) Leg 3, which helped verify theories of seafloor spreading and plate tectonics. After 50 years of advances in drilling technologies and analytical capabilities, we expect that a new transect will result in significant interdisciplinary contributions to our understanding of Earth processes. Transects of drill holes that sample both the sediment cover and the uppermost oceanic crust in a particular ocean basin can provide essential knowledge of how interconnected processes have evolved over Earth's history and responded to changes in external drivers such as atmospheric CO_2 concentrations, oceanic gateways, or major ocean currents. Transects that sample tens of millions of years of ocean crust formed at the same mid-ocean ridge (MOR) can provide important information about the duration of hydrothermal exchange. However, sampling both the sediment and the underlying basaltic basement in a specific ocean region has rarely been undertaken in a systematic manner, and the few transects accomplished cover relatively short intervals of Earth history (e.g., Juan de Fuca Ridge, 0–3.5 Ma [Shipboard Scientific Party, 1997; Expedition 301 Scientists, 2005; Expedition 327 Scientists, 2011], and Costa Rica Rift, 0–7 Ma [Anderson, Honnorez, Becker, et al., 1985]).

On average, there is a discernible conductive heat flow deficit out to 65 Ma crust (e.g., Stein and Stein, 1994), indicating that there is significant advection of heat from the cooling of the oceanic lithosphere out to this age. However, basement hydrological flow can occur in crust of all ages if sufficient hydrologic heads can be established because crustal age is only one of a suite of interlinked parameters that includes spreading rate, basement roughness, volcanic stratigraphy, and flow morphology as well as sediment type, thickness, and completeness of basement blanketing. These parameters influence the duration, depth, and intensity of off-axis hydrothermal fluid flow. Simple relationships may not exist between crustal age, fluid flow, thermal and chemical exchange, and biological activity. Figure **F2** summarizes potential relationships between these parameters.

Background

Geological setting

Expeditions 390 and 393 will operate near the DSDP Leg 3 transect (~31°S), but a new transect was selected with sites that will (1) target basement formed along the same crustal flow line at similar rates (~13–25 mm/y half rate) (Table **T1**) and (2) recover sections of slow-spreading crust of comparable ages to the ocean crust reference sections in Ocean Drilling Program (ODP) Holes 504B (7 Ma) (Shipboard Scientific Party, 1993) and 1256D (15 Ma) (Wilson et al., 2003; Expedition 309/312 Scientists, 2006; Expedition 335 Scientists, 2012), which are located in intermediate- and superfast-spreading crust, respectively. The site locations were chosen to optimize recovery of material required to achieve multidisciplinary objectives. Thicker sediment layers are frequently targeted by scientific drilling to maximize the resolution of paleoceanographic records. However, this decision has biased our sampling of in situ upper ocean crust to regions with thick sedimentary cover (for holes that penetrate >100 m into basement), which drilling as part of the SAT expeditions seeks to remediate (Figure **F3**). Rapid deposition of sediment seals crust off from the oceans, resulting in anomalously hot basement temperatures and potentially causing premature cessation of hydrothermal circulation. Consequently, most SAT target sites have sediment cover that is close to the global average thickness for their crustal age (Spinelli et al., 2004). However, because seafloor roughness is greater in slow-spreading ocean basins than in fast-spreading basins (Spinelli et al., 2004), there are significant variations in sediment thickness and the continuity of coverage along the transect. Basement crops out at all ages along

the transect (Estep et al., 2019) (Figure **F4**), and these topographic variations likely impact the crustal hydrogeology. Two sites lie ~6.7 km apart on crust estimated to be 61 Ma; crust at Site U1556 underlies 278 m of sediment, and Site U1557 (proposed Site SATL-56A) basalts underlie 564 m of sediment.

The sediment sections cored at the 61 Ma sites (U1556 and U1557) are expected to capture key Paleogene hyperthermals, including the Paleocene/Eocene Thermal Maximum (PETM), and the underlying basement will record the cumulative hydrothermal alteration of the uppermost crust across the entire SAT. The 7 Ma site (U1559) provides the young end-member for investigating the evolution of hydrothermal and microbiological systems with crustal age and allows comparison with similar-aged intermediate spreading rate crust from Hole 504B (Shipboard Scientific Party, 1993). The 31 Ma (proposed Site SATL-33B) and 49 Ma (U1558) sites fill critical gaps in our ocean crust and deep biosphere sampling with respect to basement age and major changes in ocean chemistry (Coggon et al., 2010). The 15 Ma site (proposed Site SATL-25A) was chosen for comparison to Hole 1256D (Wilson et al. 2003; Expedition 309/312 Scientists, 2006; Expedition 335 Scientists, 2012).

DSDP Leg 3 drilling results provide an indication of what to expect in the sedimentary columns of the SAT sites (Scientific Party, 1970). During Leg 3, 10 sites were drilled in the equatorial and South Atlantic Ocean between Senegal and Brazil, including 7 sites along a transect across the MAR that penetrated to basement (Sites 14–20). The basal sediment ages were within a few million years of the inferred magnetic anomaly ages, which is consistent with a half spreading rate of ~20 mm/y since 76 Ma. Recovery in the cored intervals was typically high (>98%), but the sediments were only spot cored, and there are significant gaps between cored intervals. The recovered cores make up an almost continuous Lower Cretaceous to Pleistocene composite stratigraphic section. All sites yielded calcareous sediments with calcareous nannoplankton and planktonic foraminifers.

Seismic studies/site survey data

The SAT is located along a crustal flow line where fracture zones are far apart, magnetic lineations are clear, and there is little disruption in seafloor bathymetry (Figure **F1**). The Crustal Reflectivity Experiment Southern Transect (CREST) cruise aboard the research vessel (R/V) *Marcus G. Langseth* in January and February 2016 conducted a detailed geophysical survey (http://dx.doi.org/10.1594/IEDA/500255) of the area, including a 1500 km multichannel seismic reflection profile from the ridge crest to the Rio Grande Rise spanning 0–70 Ma crust, two shorter ridge-crossing profiles spanning 0–7 Ma crust, and five ridge-parallel profiles. Ocean bottom seismometer profiles were acquired coincident with the ridge-parallel profiles. Gravity, magnetics, multibeam bathymetry, and backscatter data were also acquired. Figure **F4** shows seismic reflection profiles for Expedition 390C sites.

The present-day MAR axis at 30°–32°S has a well-defined axial valley with two inferred active hydrothermal vents (Schmid et al., 2019). The CREST seismic survey crossed a ridge segment that is ~100 km long and bounded to the north and south by ridge offsets ~16 to ~22 km in width. The absence of domal structures, which would represent oceanic core complexes (OCCs) formed by detachment faulting, near the ridge axis and the well-defined marine magnetic anomalies on the ridge flanks (Cande and Kent, 1995) are consistent with the accretion of Penrose-type layered magmatic crust.

Kardell et al. (2019) calculated ages and spreading rates from magnetic data acquired during the CREST cruise. Ages of the primary sites are estimated at 6.6, 15.2, 30.6, 49.2, and 61.2 Ma with half spreading rates of 17.0, 25.5, 24.0, 19.5, and 13.5 mm/y, respectively (Table **T1**). If 20 mm/y is used to separate slow and intermediate spreading rates (Perfit and Chadwick, 1998), then the primary sites were emplaced at both slow and intermediate spreading rates.

Seismic imaging along the CREST transect shows, at all ages from 0 to 65 Ma, an abundance of unsedimented, exposed basement outcrops that may allow the ingress and egress of seawater and ridge flank hydrothermal fluids. This suggests that the crust is never fully sealed by sediment at these ages (Estep et al., 2019) and that there may be long-lived and ongoing connection between the oceans and uppermost basaltic crust with implications for biogeochemical exchanges and subsurface microbial activity. All primary and alternate sites are positioned in localized sedimentary basins that are imaged on seismic reflection profiles. Unsedimented basement ridges are within 1–2 km of most primary sites (Figure **F4**). Sediment thicknesses were calculated using a constant sediment velocity of 1800 m/s.

Scientific objectives

The primary objective for Expedition 390C is to lay the foundation for Expeditions 390 and 393 by coring a single hole to contact with hard rock and installing reentry systems and casing at each site. By completing reentry system installations in advance, we better guarantee that the operational goals for Expeditions 390 and 393 (coring multiple APC/XCB sediment holes and drilling 250 m into basement at each site) can be achieved. For the APC/XCB hole at each site, we intended to capture the sediment/basement interface using the XCB system with a polycrystalline diamond compact (PDC) cutting shoe and advance up to 10 m into hard rock material to (a) identify the depth of the contact with hard rock and (b) recover this critical boundary for future sampling and study. The assumption was that this system may provide cleaner recovery of the interface by causing only minimal disturbance and yielding high recovery compared to rotary core barrel (RCB) coring systems. This interface is critical to documenting chemical exchange, alteration, and microbiological processes.

Because the APC/XCB cores collected during Expedition 390C will be treated as Expedition 390 and 393 samples, an additional objective of Expedition 390C was to measure ephemeral properties of the APC/XCB cores. These include in situ formation temperature measurements made with the advanced piston corer temperature (APCT-3) tool, physical properties, line scan images, X-ray images on the whole-round (WR) and split-core tracks, and paleomagnetic measurements on the archive halves. In addition, we collected one sample per core for headspace gas analysis as well as one to two WR samples per core for chemical analysis of interstitial water (IW). Geochemical data will guide chemical and microbiological sampling during Expeditions 390 and 393. A final objective was to collect samples to be distributed to micropaleontologists staffed on Expeditions 390 and 393 so a preliminary biostratigraphic age model can be developed.

Expeditions 390 and 393 have three main scientific objectives.

1. *Objective 1 (primary): quantify the timing, duration, and extent of ridge flank hydrothermal fluid-rock exchange.*

Scientific justification

Hydrothermal circulation at MORs and across their vast ridge flanks influences tectonic, magmatic, and microbial processes on a global scale; is a fundamental component of global biogeochemical cycles of key elements and isotopes (e.g., O, S, Mg, Fe, Li, B, Tl, and ^{87}Sr); and facilitates geological CO_2 sequestration within the ocean crust. The chemical and isotopic composition of seawater reflects the dynamic balance between riverine inputs from the continents, burial of marine sediments, and hydrothermal exchanges with the ocean crust (e.g., Palmer and Edmond, 1989). Ocean crust is young and chemically homogeneous compared to continental crust, and its chemical exchanges with seawater are limited to a few relatively well-known reactions. Consequently, hydrothermal contributions to ocean chemistry are simpler to reconstruct than riverine inputs (Coggon and Teagle, 2011; Davis et al., 2003; Vance et al., 2009). Knowledge of the rates and magnitudes of hydrothermal exchanges will help us to decipher the changing global conditions responsible for past variations in seawater chemistry such as mountain building, changes in seafloor spreading rate, large igneous province emplacement, changing climate, and evolution of biological systems. Building this knowledge requires ocean basin–wide transects across ridge flanks with different hydrogeologic histories.

Conductive heat flow deficits indicate that, on average, hydrothermal exchange persists at low temperatures (<<100°C) to 65 Ma on the ridge flanks (Stein and Stein, 1994). Given the vast extent of the ridge flanks, the hydrothermal fluid flux through them is many orders of magnitude greater than that through high-temperature (≤400°C) axial systems (Mottl, 2003) and is likely important for elements for which fluid-rock exchange occurs at low temperatures (e.g., Mg, K, S, Li, B, C, and H_2O). Hydrothermally altered ocean crust provides a time-integrated record of geochemical exchange with seawater manifested through changes in its chemical and isotopic composition, mineral assemblages, and physical properties (e.g., porosity, permeability, and seismic properties). The intensity of seawater-basalt exchange depends on the crustal age, architecture and thermal history, sediment cover, and spreading rate. Consequently, hydrothermal contributions to global geochemical cycles depend on the global length of slow-, intermediate-, and fast-spreading ridges and the age-area distribution of the ridge flanks, which varied significantly throughout the Phanerozoic (Müller et al., 2008). However, the impact of these variations on geochemical cycles is uncertain because the magnitude and spatial and temporal distribution of crust-seawater hydrothermal exchanges are poorly quantified. For example, the role of MOR spreading in controlling past atmospheric CO_2 and hence climate remains controversial (Alt and Teagle, 1999; Berner et al., 1983; Gillis and Coogan, 2011; Staudigel et al., 1989) because of uncertainties regarding the rate, extent, and duration of hydrothermal $CaCO_3$ precipitation due to our sparse sampling of intermediate age ocean crust (Figure **F5**). The hydrothermal carbonates that sequester CO_2 in the ocean crust also record the composition of the fluids from which they precipitate (Coggon et al., 2004) and provide an exciting opportunity to develop medium-resolution records of past ocean chemistry (e.g., Mg/Ca and Sr/Ca) (Coggon and Teagle, 2011; Coggon et al., 2010; Rausch et al., 2013), which integrates past changes in major Earth system processes such as plate tectonics, mountain building, and climate. However, this approach is limited by sparse sampling of ocean crust of a variety of ages.

Drilling experiments on the Juan de Fuca Ridge flank were a key investigation of hydrothermal evolution across a ridge flank but were restricted to young (<3.6 Ma), intermediate-spreading (29 mm/y half spreading rate) crust (Shipboard Scientific Party, 1997; Expedition 301 Scientists, 2005; Expedition 327 Scientists, 2011). There is a dearth of holes in 20–120 Ma intact in situ MOR crust and no significant penetrations (>100 m) of 46–120 Ma crust (Figure **F5**) (Expedition 335 Scientists, 2012). Consequently, the critical thermal, hydrogeologic, chemical, and microbial transitions across the ridge flanks remain unknown (Figure **F2**). Our current sampling of in situ upper ocean crust (>100 m) is biased toward areas with anomalously thick sediment for their crustal ages (Figure **F3**), and the majority of holes in ocean crust older than 35 Ma penetrate intermediate- or fast-spreading crust. The recovery of uppermost basement sections along the SAT across slow/intermediate-spreading MAR crust will address these sampling gaps with respect to age, spreading rate, and sediment thickness.

Crustal accretion along the northern MAR is complex, and there are significant regions where spreading is accommodated by amagmatic extension by detachment faults that exhume sections of deep lithosphere to form OCCs (Mallows and Searle, 2012). However, a recent survey of the modern southern MAR during Cruise MSM25 of the R/V *Maria S. Merian* (2013) found no OCCs between 25°S and 33°S (Devey, 2014). This, combined with the relatively well defined marine magnetic anomalies on the southern MAR flanks (Maus et al., 2009), is consistent with accretion of intact magmatic crust. Because the ~31°S SAT follows a crustal flow line through a relatively long spreading segment (~100 km) away from major transform faults, we expect a Penrose-type stratigraphy of lavas overlying dikes and gabbros to have been accreted along the transect (Penrose Conference Participants, 1972).

Expected outcomes

Hydrothermal alteration of basement cores will be investigated using a combination of petrological and geochemical analyses, radiometric dating, and detailed quantitative core logging of rock types, alteration features, and veins. The recovery of thinly sedimented slow/intermediate-spreading ocean crust along the proposed SAT will provide the following opportunities:

- To determine the nature, rates, magnitudes, distribution, and duration of hydrothermal alteration across the ridge flank;
- To investigate the effect of titanomagnetite/titanomaghemite alteration on the magnetic anomaly signal to elucidate its origin;
- To compare hydrothermal alteration of the uppermost slow/intermediate-spreading crust with crust of similar ages produced at faster spreading ridges (e.g., Holes 504B and 1256D);
- To evaluate the effect of changes in global spreading rates and the age-area distribution of the seafloor on hydrothermal contributions to global biogeochemical cycles; and
- To investigate signatures of changing ocean chemistry in the hydrothermal record and develop medium-resolution records of past ocean chemistry using hydrothermal minerals (following Coggon et al., 2010).

It will also allow us to test the following hypotheses:

- Hydrothermal chemical exchange ceases within 20 My of crustal formation.
- Basement topography and sedimentation history affect the rate and duration of hydrothermal alteration.

2. *Objective 2 (primary): investigate sediment- and basement-hosted microbial community variation with substrate composition and age*

Scientific justification

Scientific ocean drilling has revealed that microorganisms, Archaea, Bacteria, and eukaryotic fungi and protists are present, intact, and metabolically active in uncontaminated deep subsurface sediment and basalt. Knowledge about subseafloor microbial communities has grown exponentially since the initial microbial investigations by DSDP in the 1980s, but <4% of ODP/Integrated Ocean Drilling Program/IODP sites sampled have been sampled, documented, or archived for microbiological purposes (Kallmeyer et al., 2012; Orcutt et al., 2014). Determining microbial community composition and physiological capabilities along the SAT will provide insights into the role of microbes in mineral alteration, hydrocarbon formation, and global biogeochemical cycles.

In sediments, the number of microbial cells present is estimated to equal that in the entire oceanic water column (Kallmeyer et al., 2012). However, the amount of biomass stored in the deep subsurface remains contentious because microbial cell abundance in subseafloor sediment varies by approximately five orders of magnitude with significant geographic variation in the structure of subseafloor communities (Inagaki et al., 2006). The majority of studies have focused on relatively high biomass continental shelf systems (Inagaki and Orphan, 2014). Recent efforts, including Integrated Ocean Drilling Program Expeditions 329 (South Pacific Gyre; Expedition 329 Scientists, 2011) and 336 (North Pond; Expedition 336 Scientists, 2012), investigated lower biomass sedimentary systems underlying oceanic gyres. Crucially, no data have been collected from the South Atlantic Gyre. Such data would refine the global biomass census and improve our understanding of the global carbon cycle.

The presence or absence of oxygen in marine sediments has profound implications for the quantity, diversity, and function of microbial communities. Oxygen penetration depth varies between oceanic regions and settings, ranging from only a few millimeters in areas with high rates of microbial respiration, such as on continental shelves, to the entire sediment column in extremely low biomass sediments, such as those beneath the South Pacific Gyre (D'Hondt et al., 2015). Extrapolation of an observed global relationship between oxygen penetration and sedimentation rate and thickness indicates SAG sediment may be oxic to basement (D'Hondt et al., 2015). During Leg 3, oxygen was not measured, but sulfate was detected near the basement. However, sediment organic carbon concentrations along the SAT are intermediate to those of North Pond, where oxygen penetrated tens of meters below seafloor and nitrate was present to basement, and Nankai Trough, where oxygen was depleted by 3 meters below seafloor (mbsf) and sulfate was depleted by 19 mbsf (Expedition 336 Scientists, 2012; Tobin et al., 2009; Orcutt et al., 2013; Reese et al., 2018). This indicates that oxygen is unlikely to extend to the basement at sites along the SAT, contrary to model predictions (D'Hondt et al., 2015), and that the classical redox succession of oxygen respiration followed by nitrate reduction, potentially followed by metal reduction, may be present. However, we hypothesize that oxygen will be reintroduced at the bottom of the sediment column as a result of oxygenated fluid flow in the uppermost volcanic basement, which is the case at North Pond (Expedition 336 Scientists, 2012). The recovery of the sediment package will allow us to address this conundrum regarding oxygen penetration, biomass, and carbon limitation of microbial activity.

We will compare the phylogenetic diversity, functional structure, and metabolic activity of SAG communities with results from previously studied regions. By exploiting the variations in sediment carbon composition expected across the subsiding MOR flank, we can examine the response of autotrophy versus heterotrophy to carbonate chemistry. Additionally, previous studies of the sedimentary deep biosphere have explored community diversity based on site-to-site or downhole (age) comparisons, often implicitly assuming a similar "starter community" that colonized the seafloor and whose structure and function subsequently changed in response to evolving geochemical conditions or burial depth. However, recent work suggests energy limitation may preclude replication (Lever et al., 2015; Lomstein et al., 2012) and thus limit community changes. The proposed age-transect approach will allow us to test this assumption directly by investigating the impact of burial depth and chemical zonation on sediment of the same age and hence the same starter community.

Given the dearth of basement holes in ocean crust of intermediate age, there are no microbiological samples across the critical ridge–flank transitions in basement properties that may affect microbial communities (Figure **F2**). The majority of biological alteration of subseafloor basalts is thought to occur within 20 My of crustal formation (Bach and Edwards, 2003). However, microbiological investigations of oceanic basement have focused on young (<10 Ma) crust (Jungbluth et al., 2013; Lever et al., 2013; Mason et al., 2010; Orcutt et al., 2011) or older (>65 Ma) lava associated with hotspot volcanism along the Louisville Seamount Trail (Expedition 330 Scientists, 2012; Sylvan et al., 2015). Basement outcrops that penetrate the relatively impermeable sediment provide permeable conduits that facilitate subseafloor fluid circulation in older basement (Wheat and Fisher, 2008). Fluid flow across the sediment/basement interface can produce redox gradients that provide recharge of depleted electron acceptors (e.g., oxygen and nitrate) to basal sediments, as observed above 3.5 and 8 Ma ocean crust on the Juan de Fuca Ridge flank (Engelen et al., 2008) and at North Pond (Orcutt et al., 2013), respectively. However, the extent and duration of fluid flow through this interface across the ridge flanks remains unknown (Figure **F2**). The recovery of the uppermost basaltic basement from 7 to 61 Ma along the SAT will allow us to determine whether microbial populations are indeed present in basement older than 20 Ma and to investigate the nature, extent, and duration of communication between the sedimentary and crustal biosphere for the first time.

Expected outcomes

We will sample subseafloor populations of Bacteria, Archaea, and microbial eukaryotes in both the sedimentary and upper crustal ecosystems along the proposed transect, quantify their biomass by cell enumeration, identify them using molecular biology methods, measure the stable isotopic composition (C, N, and S) of sediment and basement to relate processes to geochemistry, measure their metabolic activities using a variety of incubation assays, and resolve their physiological adaptations with omics-based approaches with the following aims:

- To evaluate cell abundance and community activity in the low-energy subseafloor biosphere of the SAG and refine estimates of global subseafloor sedimentary microbial abundance;
- To resolve model predictions about the depth of oxygen penetration into sediment from overlying seawater and into the bot-

tom of the sediment package from oxygenated fluid in basement;
- To evaluate the role of subseafloor microbes in sediment biogeochemistry and basement alteration and hence global biogeochemical cycles; and
- To investigate how aging of the ocean crust influences the composition of the crustal biosphere, particularly the effects of changing oxidation state and permeability on microbial abundance, diversity, and function.

Our samples will also allow us to test the following hypotheses:

- SAG microbial communities share membership and function with both oligotrophic sediments, like those found at North Pond, and open ocean systems with higher organic matter input, such as the Nankai Trough, given the intermediate organic carbon content of the SAT sites.
- Microbial community structure and diversity depend on the starter community (and hence sediment age) rather than subsequent selection driven by burial or chemical zonation.
- Crustal biomass decreases with increasing basement age, and communication between the sedimentary and crustal biosphere ceases within 20 My.
- Microbial diversity increases within subseafloor basalts with basement age as previously demonstrated in basalts exposed on the seafloor (Lee et al., 2015; Santelli et al., 2009).

3. *Objective 3 (secondary): investigate the responses of Atlantic Ocean circulation patterns and the Earth's climate system to rapid climate change including elevated atmospheric CO_2 during the Cenozoic*

Scientific justification

Climate change due to increased atmospheric CO_2 poses significant and imminent threats to global society and the environment. Knowledge of past ocean circulation patterns and temperatures is required to assess the efficacy of numerical models in simulating intervals of high pCO_2. High pCO_2 intervals are often characterized by relatively shallow lysocline and calcite compensation depths (CCDs) resulting in poor preservation of $CaCO_3$ microfossils used to reconstruct paleoceanographic records. This problem can be overcome by coring sediment deposited on basement slightly older than the targeted sediment age that accumulated prior to thermal subsidence of the seafloor below the CCD. More continuous composite stratigraphic sequences are obtained by drilling multiple sites along a crustal age transect, a strategy successfully employed during ODP Leg 199 (Shipboard Scientific Party, 2002) and Integrated Ocean Drilling Program Expedition 320/321 (Pälike et al., 2012). The Walvis Ridge depth transect sampled during ODP Leg 208 demonstrated the dynamic nature of the Cenozoic CCD and lysocline in the southeastern Atlantic (Shipboard Scientific Party, 2004) and the value of redrilling previous transects to collect more complete records of Earth's history. Although spot cored, Leg 3 sites demonstrate moderate to excellent carbonate preservation along the SAT (Scientific Party, 1970) and the location's suitability for high-resolution paleoclimatic and paleoceanographic reconstructions through key intervals of rapid climate change (Cramer et al., 2009; Zachos et al., 2001, 2008), including the PETM and other short-lived hyperthermals, early and middle Eocene climatic optima, the onset of Antarctic glaciation across the Eocene/Oligocene boundary (Oi1 event), multiple Oligocene and Miocene glaciation events (Oi and Mi events), the Miocene climatic optimum and Monterey Carbon Excursion, Pliocene warmth, and the onset of Northern Hemisphere glaciation.

Global ocean circulation transfers heat and nutrients around the globe, both influencing and responding to changes in Earth's climate system (Broecker, 1991; Stommel, 1961; Wunsch, 2002). Fortuitously, the western intensification of ocean currents means we can substantially reconstruct deepwater mass properties and thus thermohaline circulation history by characterizing western portions of major ocean basins using drilling transects. The western South Atlantic is the main northward flow path of Antarctic Bottom Water and southward flow path of North Atlantic Deep Water and their precursor water masses. Consequently, the SAT cores will provide complementary data needed to constrain the evolution of thermohaline circulation patterns and climate change as the Drake Passage and Southern Ocean opened, the northern North Atlantic deepwater gateway opened, and the Tethys Ocean became restricted to thermohaline circulation. In particular, these cores will assist in establishing how high-latitude sea surface (and hence deep ocean) temperatures and the CCD varied in response to pCO_2 changes and ocean acidification (Barker and Thomas, 2004; Barrera et al., 1997; Billups, 2002; Bohaty et al., 2009; Cramer et al., 2009; Frank and Arthur, 1999; Kennett and Stott, 1991; Scher and Martin, 2006; Thomas et al., 2003; Wright et al., 1991, 1992). The SAT will yield a complementary record to western North Atlantic sediments (Expedition 342; Norris et al., 2014), and together these data will provide an exceptional record of the evolution of Atlantic overturning circulation through the Cenozoic.

A novel, direct way to compare paleoceanographic reconstructions of past high pCO_2 to modern conditions is to recover sediments along transects of water column data collected by the World Ocean Circulation Experiment (WOCE). The SAT constitutes a "paleo-WOCE" line following the western portion of WOCE Line A10 (Figure **F1**), providing access to paleoceanographic records of southern- and northern-sourced deep and bottom waters. We will test models of bipolar deepwater evolution (e.g., Borelli et al., 2014; Cramer et al., 2009; Katz et al., 2011; Tripati et al., 2005) using stable and radiogenic isotope analyses of sediments recovered from these key western South Atlantic sites.

The Walvis Ridge depth transect (Shipboard Scientific Party, 2004) revealed a dramatic 2 km CCD shoaling during the PETM due to the acidification of the ocean from massive carbon addition followed by a gradual recovery (Zachos et al., 2005; Zeebe et al., 2008). Given chemical weathering feedbacks, the recovery of the CCD should have resulted in a transient overdeepening of the CCD (Dickens et al., 1997). Collectively, the SAT sites will provide additional data for reconstructing changes in the position of the lysocline and CCD in the western South Atlantic that are essential for constraining the timing of gateway events and the history of Northern Component Water and Southern Component Water, which were the precursors to North Atlantic Deep Water and Antarctic Bottom Water, and the nature of Atlantic basin responses to climate change relative to the Pacific.

Expected outcomes

Microfossils provide a critical archive of ocean and climate history, including long-term changes (e.g., early Eocene warmth, Cenozoic cooling, and Pliocene warmth) and abrupt events (e.g., early Paleogene hyperthermals and multiple glaciation events). Complete sedimentary sections recovered along paleo-WOCE Line A10 will exploit thermal subsidence of the ocean crust along the transect to provide material for high-resolution proxy records includ-

ing benthic and planktonic foraminiferal geochemistry, micropaleontological assemblages, orbitally tuned age models, neodymium isotopes, and alkenone $\delta^{13}C$ and boron isotope pCO_2 reconstructions with the following aims:

- To reconstruct the evolution of deepwater masses over the past 61 My to assess contributions of Northern Component Water and Southern Component Water in the early Paleogene western South Atlantic (Kennett and Stott, 1990) and to document the influence of the openings of the Drake and Tasman Passages on South Atlantic deepwater circulation;
- To provide high-resolution constraints on CCD and carbonate chemistry changes of the deep western Atlantic, particularly during transient hyperthermals and other intervals of global warmth;
- To reconstruct the Cenozoic history of the South Atlantic subtropical gyre by monitoring proxies of productivity and paleobiogeography of oceanic plankton, rates of speciation/extinction relative to those of the equatorial zone and higher latitudes, and changes in biodiversity and subtropical ecosystem dynamics; and
- To evaluate the response of subtropical planktonic and benthic biota to changing environmental conditions such as global warming, ocean acidification, or fertility patterns during intervals of rapid climate change through the Cenozoic.

Drilling at these sites will also allow us to test the following hypotheses:

- Low-latitude sites were potential sources of deep water formation at times of global warmth and high atmospheric pCO_2.
- The strength of the coupling between the climate and the carbon cycle varied through the Cenozoic.
- The lysocline and CCD responded differently on the western side of the MAR compared to the Walvis Ridge record due to changing deep/bottom water sources, gateway configurations, and flow paths.
- The subtropical gyre cut off the delivery of heat to Antarctica as the Antarctic Circumpolar Current developed through the late Eocene–Oligocene.

Site summaries

Beginning of expedition and transit

Expedition 390C started in Kristiansand, Norway, at 0800 h (UTC + 2 h) on 5 October 2020 with the arrival and boarding of 18 *JOIDES Resolution* Science Operator (JRSO) personnel on the *JOIDES Resolution*. Two additional JRSO staff were already on board. Three JRSO staff crossed over and departed on the same day. There was no science party on Expedition 390C.

All arriving personnel followed preboarding protocols to mitigate the risk of a COVID-19 infection on the ship, including a 2 week shelter-in-place period prior to travel, a pretravel COVID-19 test, and a 5 day quarantine in a hotel in Kristiansand. Personnel passed three additional COVID-19 tests during this quarantine. Shipboard personnel wore masks and followed social distancing protocols during the COVID-19 mitigation period.

The vessel had been tied up for over 1 month (Expedition 390P), during which time the Schlumberger wireline winch heat exchanger was replaced. During port call, final maintenance and deliveries were completed, including the delivery of new asbestos-free brake bands for the drawworks.

The ship departed Kristiansand on 7 October, and the last line was released at 0918 h. The transit from Kristiansand to Site U1556 was undertaken in two legs. First, the ship transited to Las Palmas, Canary Islands (Spain) for a refueling stop. The voyage took 182.85 h (7.6 days) and covered 2144 nmi at an average speed of 11.7 kt. The ship anchored in Las Palmas at 2306 h on 14 October and fueling began at first light on 15 October. The ship received 1113.6 mt of fuel oil. While at anchorage, a repaired propulsion motor was recoupled and put back online. Siem Offshore crew tested and maintained the release hooks of the two port lifeboats, lowering them to the waterline and recovering them. The ship was underway again by 1454 h. COVID-19 risk mitigation policies were lifted upon departure because it had been more than 14 days since the last possible exposure. The transit from Las Palmas to Site U1556 in the South Atlantic Ocean took 299.5 h (12.5 days) at an average speed of 12.2 kt and covered 3608 nmi.

Site U1556

Background and objectives

Site U1556 (proposed Site SATL-53B) is in the central South Atlantic Ocean, ~1250 km west of the MAR. The objective for Expedition 390C was to core one hole with the APC/XCB system to basement for gas safety monitoring and to install a reentry system with casing through the sediment to ~5 m into basement in a second hole to expedite basement drilling during SAT Expeditions 390 and 393.

Site U1556 is located on Seismic Line CREST1A/B at common depth point (CDP) 3410 near the CREST05 crossing line. A reflector at ~6.9 s two-way traveltime (TWT) was interpreted to be the top of basement and estimated to be at 180 mbsf (Figure **F4**). The reflector marks a change in seismic character from high-frequency layered energy to low-frequency chaotic energy. This site is located only 6.7 km from Site U1557, and the basement at both sites is predicted to be ~61.2 Ma and formed at a half spreading rate of ~13.5 mm/y. Oceanic crust at these sites is the oldest that will be drilled as part of the SAT expeditions and will be compared to younger crustal material. The contrasting sediment thicknesses at these closely spaced sites, with Site U1556 being less heavily sedimented, will allow exploration of the effect of sediment thickness on crustal evolution. Overlying sediment from Site U1556 is expected to be primarily carbonate ooze and will be used in paleoceanographic and microbiological studies. Average sediment accumulation rate at this site was predicted to be only 2.9 m/My, the lowest of all sites along the proposed SAT. As such, microbiological research at this site will provide insight into how subsurface microbial communities underneath the low-nutrient South Atlantic Gyre survive.

Operations

The *JOIDES Resolution* arrived at Site U1556 at 0206 h on 28 October 2020. We switched from cruise mode to dynamic positioning (DP) mode at 0230 h and started operations for Hole U1556A. No acoustic beacon was deployed. Hole U1556A is located at 30°56.5244'S, 26°41.9472'W, and the water depth is 5006.4 meters below sea level (mbsl). The APC/XCB bottom-hole assembly (BHA) was made up and deployed. A nonmagnetic drill collar was used above the outer core barrel to improve the quality of magnetic orientation data collected during APC coring. We lowered the drill bit to 5006 mbsl and pumped a "pig" (pipe cleaning device) through the drill string to remove rust. At ~2200 h on 28 October, the sinker bars and core orientation tool were installed and the core barrel was lowered. We spudded Hole U1556A at 2300 h. Mudline Core 390C-

U1556A-1H arrived on deck at 2335 h and recovered 9 m. Cores 1H–16H advanced to 151.4 mbsf and recovered 155.13 m (103%). All APC cores were oriented with the Icefield MI-5 core orientation tool following new procedures to identify any rotation relative to the core barrel during deployment. Formation temperatures were measured on Cores 4H, 7H, 10H, and 13H with the APCT-3 tool. Cores 11H–13H were partial strokes due to the stiffness of the sediment but had good recovery; Cores 14H and 15H were full strokes. Core 16H experienced 60 klb overpull and had to be drilled over to release it from the formation. Consequently, we changed to the XCB coring system using the PDC cutting shoe. Cores 17X–29X advanced from 151.4 to 273.6 m and recovered 79.53 m (65%). The rate of penetration was <10 m/h for Cores 17X–20X and increased to an average of 15.2 m/h for Cores 21X–29X.

Core 390C-U1556A-30X encountered a hard layer that decreased the rate of penetration dramatically. Upon recovery, this layer was confirmed to be hard rock and was determined to be at 278 mbsf. Cores 31X–33X attempted additional coring of the altered basalt and volcaniclastic material. In total, Cores 30X–33X advanced 5.8 m into basement and recovered 4.33 m (75%), reaching a total depth of 283.8 mbsf. The sediment/basement interface in Core 30X had the lowest recovery (23%), but we experienced higher recovery in subsequent cores (90% for Cores 31X–33X) (Figure **F6**). Core quality was also high, with the XCB PDC cutting shoe returning nicely trimmed and relatively large pieces. We observed minimal wear on the cutting shoe.

In summary, Hole U1556A reached a total depth of 283.8 mbsf and recovered 243.78 m (86%), taking 4.1 days of expedition time (Table **T2**; Figure **F7**). Following recovery of Core 33X, we raised the pipe to ~20 m above seafloor. The seafloor was cleared at 0410 h, ending Hole U1556A. We then transited in DP mode to nearby Site U1557 to conduct APC/XCB coring there. The intention was to core to basement at Site U1557 and then return to Site U1556 to install a reentry system with casing. However, the failure of the subsea camera system at Site U1557 made it impossible to complete the planned reentry system installation at Site U1556. Thus, the end of Hole U1556A was also the end of Site U1556 for Expedition 390C.

Principal results

Basement was found to be deeper than expected at Site U1556 based on the initial interpretation of seismic data (278 instead of 180 mbsf). A lower reflector at ~6.95 s TWT is now identified as the sediment/basement interface (Figure **F4**). This basement depth also increases the average sediment accumulation rate to 4.5 m/My from the original estimate of 2.9 m/My (Table **T1**).

Cores 390C-U1556A-1H through 29X were measured on the WR and split-core track systems. We collected physical properties data, line scan optical images, X-ray images, and paleomagnetic measurements. Basement Cores 30X–33X were measured on the WR track systems but were not split; they were preserved in nitrogen gas–flushed bags for description and analysis during Expeditions 390 and 393. Core catcher samples were collected for postexpedition biostratigraphic dating. In addition, we collected one sample per core for headspace gas analysis as well as one to two WR samples per core for chemical analysis of IW. Starting with Core 17X, we collected 10 cm instead of 5 cm WR samples to ensure enough water was available for standard analyses. No systematic core description took place during Expedition 390C. Sediment lithology in Hole U1556A alternates between 1 and 10 m thick layers of red-brown clay and carbonate ooze with sharp contacts between these lithologies. Analysis of calcium carbonate content conducted on samples from IW squeeze cakes also demonstrates this alternation. Calcium carbonate content ranges from a minimum of 0.08 wt% in clay to 92.08 wt% in carbonate ooze. Physical properties data reflect similar lithologic changes, with higher magnetic susceptibilities and counts of natural gamma radiation (NGR) in the clay layers. *P*-wave velocity and gamma ray attenuation (GRA) bulk density increase downhole with a significant increase in both in basement cores. APCT-3 formation temperature measurements from Cores 4H, 7H, 10H, and 13H ranged from 3.1°C to 6.2°C and had a good linear fit.

Alkalinity generally decreases downhole, although a broad peak in concentration at intermediate depths (~150 mbsf) and a secondary peak at ~220 mbsf may reflect sulfate reduction. Total dissolved sulfur concentrations, as measured using inductively coupled plasma atomic emission spectrometry (ICP-AES) of IW samples, decrease toward this depth and then level out, not decreasing below 22 mM even at the bottom of the hole. Sulfate concentrations measured by ion chromatography reveal the same trend but are noisier than the ICP-AES data. Peaks in dissolved manganese and ammonium in the upper half of the hole also indicate active reductive processes and heterotrophic metabolisms. Dissolved iron was below the detection limit, likely because it reoxidized and precipitated during the WR squeezing process. Dissolved silicon and boron are inversely correlated, with a sharp peak in silicon concentrations at an intermediate depth (~151 mbsf) coinciding with a sharp decline in boron. Calcium and strontium concentrations reach a broad peak at an intermediate depth and are lower in the upper and lower parts of the hole. Magnesium and potassium, conversely, are highest in surface samples, decrease with depth, and then increase again slightly near basement. This increase may suggest fluid flow along or near the sediment/basement interface.

All cores excluding the unsplit basement sections were measured on the superconducting rock magnetometer (SRM) for natural remanent magnetization (NRM) and then at alternating field demagnetization levels of 5, 10, and 20 mT. Vertical drilling overprints were ubiquitous but were generally removed by the 5 mT demagnetization step. Many samples appear to show a characteristic remanent magnetization (ChRM) after 20 mT demagnetization, although some likely have a higher coercivity component that will need to be examined during postexpedition research. APC cores were magnetically oriented, and a correction was applied to the SRM data for each core. Corrected declinations roughly cluster around two antipodal locations, assuming a geocentric axial dipole and some level of paleosecular variation.

Site U1557

Background and objectives

Site U1557 (proposed Site SATL-56A) is in the central South Atlantic Ocean, ~1250 km west of the MAR. The objective for Expedition 390C is to core one hole with the APC/XCB system to basement for gas safety monitoring and to install a reentry system with casing through the sediment to ~5 m above basement in a second hole to expedite basement drilling during SAT Expeditions 390 and 393.

Site U1557 is located on Seismic Line CREST1A/B at CDP 4470 near the CREST05 crossing line. A reflector at ~7.2 s TWT was interpreted to be the top of basement and estimated to be at 510 mbsf (Figure **F4**). This site is located only 6.7 km from Site U1556, and the basement at both sites is estimated to be ~61.2 Ma, formed at a half spreading rate of ~13.5 mm/y. Oceanic crust at these sites is the oldest that will be drilled as part of the SAT expeditions, and it will

be compared to younger crustal material. The contrasting sediment thicknesses at these closely spaced sites, with Site U1557 being more heavily sedimented, will allow exploration of the effect of sediment thickness on crustal evolution. Overlying sediment from Site U1557 is expected to be primarily carbonate ooze and will be used in paleoceanographic and microbiological studies. The thick sediment layers at this site in particular will allow for paleoceanographic records covering the entire Cenozoic to be developed, including reconstruction of Atlantic Ocean circulation patterns during periods of elevated CO_2 during the Cenozoic.

Operations

We opted to core and install a reentry system at proposed alternate Site SATL-56A instead of proposed primary Site SATL-54A because the thinner sediment layer (estimated to be 510 m thick at Site SATL-56A and 640 m at Site SATL-54A) would allow installation of casing to basement. Stress calculations indicated that casing could only be installed to 600 m without exceeding the safe utilization threshold of the drill pipe. The reentry system and casing installation was planned as two stages. First, the reentry cone and five joints of 16 inch casing would be jetted in to ~60 mbsf, and 10¾ inch casing string would then be drilled into basement.

Hole U1557A

We arrived at Site U1557 on 1 November 2020 after moving the ship in DP mode 6.7 km east from Site U1556 at an average speed of 0.9 kt with the APC/XCB BHA and bit suspended ~20 m above seafloor. There was no acoustic beacon deployed. Hole U1557A is located at 30°56.4549'S, 26°37.7912'W. The bit was lowered to 5003.9 mbsl for the first core based on the expected precision depth recorder seafloor depth of 5011.3 mbsl. The first mudline core came back empty. A second mudline core was attempted from a water depth of 5009.9 mbsl and also came back empty. The drill string was lowered to 5011.9 mbsl for a third attempt. Core 390C-U1557A-1H overpenetrated and came back with a full core barrel. We thus ended Hole U1557A and offset the ship 20 m east to begin Hole U1557B.

Hole U1557B

Hole U1557B is located at 30°56.4547'S, 26°37.7775'W. The hole was spudded at 1615 h on 1 November 2020 from a drill string depth of 5006.9 mbsl. Core 390C-U1557B-1H recovered 4.1 m of sediment and established the seafloor depth as 5012.3 mbsl. Cores 1H–11H advanced to 99.1 mbsf and recovered 90.95 m (92%). All APC cores were taken with a nonmagnetic core barrel and oriented with the Icefield MI-5 core orientation tool following new procedures to identify any rotation relative to the core barrel during deployment. Formation temperatures were measured on Cores 4H, 7H, and 10H using the APCT-3 tool. Cores 2H and 3H had lower recovery than expected for APC coring of surface sediment (68% and 43%, respectively); this result may be explained by one or more hard layers near the surface that we were not able to recover. Core 11H had to be drilled over to release it from the formation. Consequently, the decision was made to switch to the XCB coring system with the PDC cutting shoe.

XCB coring continued smoothly. Cores 390C-U1557B-12X through 62X advanced from 99.1 to 562.4 mbsf and recovered 317.35 m (68%). The sinker bars were removed after a hard layer was encountered at 239 mbsf. The rate of penetration for Cores 12X–44X averaged 14.6 m/h. Starting with Core 45X, the rate of penetration decreased substantially in increasingly hard sediment, averaging 5.8 m/h for Cores 45X–62X. We began conducting mud sweeps with Core 61X and continued mud sweeps on every core thereafter. Hard rock was encountered at 564 mbsf in Core 63X. Three additional XCB cores were taken to achieve 10 m penetration into basement. Cores 64X and 65X had low recovery (<50%), and Core 64X consisted of small rubbly pieces that appeared to jam in the core liner and core catcher. Core 66X had 100% recovery on a 2.1 m advance (drilled by time) and returned cohesive pieces of basalt/breccia (Figure **F6**). Overall, coring in Hole U1557B advanced to 574.0 mbsf and recovered 414.94 m (72%), taking 7.5 days of operational time (Table **T2**; Figure **F7**). As at Site U1556, the XCB PDC cutting shoe performed extremely well in Hole U1557B, returning cohesive pieces of hard rock and showing minimal wear. Coring in basement was deliberately kept to 2 h per core, after which the core was pulled and the cutting shoe was inspected for integrity. No cutters were observed to be lost or damaged.

After Core 66X was recovered, we prepared for a jet-in test to determine whether sediment at Site U1557 was appropriate for the installation of a reentry cone and five joints of 16 inch casing (~60 m) prior to installation of 10¾ inch casing to basement. We pulled out of the hole to ~30 m above seafloor, and the bit cleared the seafloor at 0210 h, ending Hole U1557B.

Hole U1557C

The ship repositioned 20 m south for the jet-in test, and Hole U1557C was spudded at 0345 h on 9 November 2020 with the APC/XCB BHA. The jet-in test advanced to 3 m before contacting a hard layer, and we were unable to jet in farther despite increasing the flow rate. The ship was repositioned 20 m west for a second jet-in test that was also unable to penetrate the seafloor. Because the jet-in tests were unsuccessful, the top drive was set back and the drill string was pulled back to the surface. The bit cleared the rig floor at 1930 h, ending Hole U1557C. This experience provides additional evidence for one or more surface hard layers at this site.

Hole U1557D

A revised plan was made to drill in the reentry cone with five joints of 16 inch casing (~60 m) using a stinger with a mud motor, underreamer, and drill bit (Figure **F8**). In preparation for assembling the casing string, the mouse hole and upper guide horn (UGH) were removed and the reentry cone was moved under the rotary table on top of the moonpool doors. The casing was made up, lowered through the reentry cone, and latched into the hanger. The first three joints were locked and welded. We then tested the mud motor and underreamer to determine the pump rate required to open up the arms of the underreamer (50 strokes/min and 350 lb/inch^2). The full casing stinger was assembled with a 14¾ inch bit and lowered through the reentry cone. The Dril-Quip running tool at the top of the stinger was latched into the reentry cone. The driller lifted the assembly, measuring the weight of the reentry system and checking the engagement of the running tool. The moonpool doors were opened, and the reentry cone, casing, and stinger assembly were lowered through the splash zone at 1045 h on 10 November 2020. The reentry system was lowered using a controlled descent to 729.0 meters below rig floor (mbrf) while filling the drill pipe with water every 10 stands, and the UGH was reinstalled before we continued lowering the drill string.

When the reentry cone reached ~4020 mbsl, the subsea camera system was deployed and lowered quickly until it caught up with the cone. The camera then began following the cone down. At 0615 h on 11 November and at ~4900 mbsl, video feed and communication

from the subsea camera system was lost and the system was pulled back to the surface to diagnose and repair the issue. The telemetry pod was swapped out for a spare and the system redeployed. At the same depth (~4900 mbsl), video and communication were again lost, and the system was pulled back to the surface. In the meantime, Hole U1557D was spudded at 1050 h on 11 November, and the reentry cone and five joints of 16 inch casing were successfully drilled into the sediment to 64.2 mbsf. The driller lost the weight of the reentry system with casing at 5010.7 mbsl, establishing that depth as the seafloor depth for Hole U1557D. The Dril-Quip running tool was disconnected from the reentry cone at 1400 h, without the ability to observe this operation on the subsea camera.

We determined that the problem with the subsea camera system was pressure related. Consequently, we were not able to complete the installation of 10¾ inch casing to basement in Hole U1557D. Instead, we decided to transit to Site U1558 and continue coring and reentry system installations at the other planned sites, where the water depth is shallower and pressure was not expected to limit use of the subsea camera.

The drill string was pulled back to the surface. The UGH was removed to recover the Dril-Quip running tool and was then reinstalled after recovery of the running tool and the BHA. The rig floor was secured at 0908 h on 12 November for the transit to Site U1558. Overall, Hole U1557D took 2.6 days of expedition time.

Principal results

After basement at Site U1556 was found to be substantially deeper than predicted, the seismic data for Site U1557 were also reinterpreted (Figure **F4**). The revised estimate was 585 mbsf instead of 510 mbsf. Basement was encountered at 564 mbsf, providing a tie point for future seismic interpretations.

Cores 390C-U1557A-1H and 390C-U1557B-1H through 62X were measured on the WR and split-core track systems. We collected physical properties data, line scan optical images, X-ray images, and paleomagnetic measurements. Basement cores were measured on the WR track systems but were not split. Instead, they were preserved in nitrogen gas–flushed bags for description and analysis during Expeditions 390 and 393. Core catcher samples were collected for postexpedition biostratigraphic dating. In addition, we collected one sample per core for headspace gas analysis as well as one WR sample per core for chemical analysis of IW. Starting with Core 390C-U1557B-19X, we collected 10 cm instead of 5 cm WR samples to ensure enough water was available for standard analyses. No systematic core description took place during Expedition 390C. Sediment lithology alternates between 1 and 10 m thick layers of clay and carbonate ooze with sharp contacts in between. Compared to Hole U1556A, in Hole U1557B clay layers are generally thinner and carbonate ooze layers are slightly thicker. After Core 32X (bottom depth = 296.1 mbsf), the lithology transitioned toward predominantly carbonate ooze with an average calcium carbonate content of 86 wt%. Rare clay layers are <1 m thick. Physical properties such as magnetic susceptibility and counts of NGR generally correlate with lithology, and higher magnetic susceptibility values and NGR counts are found in the clay layers than in the hard rock sections. *P*-wave velocity and GRA density increase downhole with a significant increase in both values in basement cores. APCT-3 formation temperature measurements from Cores in Hole U1557B U1556A-4H, 7H, and 10H ranged from 2.4°C to 4.8°C and had a relatively good linear fit.

Alkalinity is high near the top of Hole U1557B, decreases to ~75 mbsf, and then shows a generally increasing trend toward the bottom of the hole. Near basement, alkalinity spikes to 12.3 mM but declines again in the final IW sample collected before reaching hard rock material. Total dissolved sulfur concentrations, as measured using ICP-AES of IW samples, decrease downhole from surface levels then level out. A sharp decrease in concentration (from ~24 to 19.5 mM) is associated with the increase in alkalinity near the bottom of the hole. Sulfate concentrations measured using ion chromatography closely match the sulfur data measured using ICP-AES. Nonetheless, sulfate concentrations remain above 20 mM even at the bottom of the hole. Peaks in dissolved manganese and ammonium in the upper half of Hole U1557B also indicate active reductive processes and heterotrophic metabolisms. A secondary dissolved manganese peak occurs at an intermediate depth. Dissolved iron was below the detection limit, likely because it reoxidized and precipitated during the WR squeezing process. Dissolved silicon and boron are inversely correlated throughout most of the hole, with a sharp peak in dissolved silicon concentrations in the upper half of the hole coinciding with a sharp decline in boron. The depth of this peak (~168 mbsf) is approximately the same as the depth of the peak in silicon concentrations observed in Hole U1556A (~151 mbsf). Near the bottom of the hole, both dissolved silicon and boron concentrations increase sharply but decline again immediately before reaching basement. Calcium and strontium concentrations reach a broad peak at an intermediate depth and are lower in the upper and lower parts of the hole top. Magnesium and potassium, conversely, are highest in surface samples, decrease with depth, and then increase again slightly near basement. This increase may suggest fluid flow along or near the sediment/basement interface.

All cores excluding the unsplit basement sections were measured on the SRM for NRM and then at alternating field demagnetization levels of 5, 10, and 20 mT. Vertical drilling overprints were ubiquitous but were generally removed by the 5 mT demagnetization step. Many samples appeared to show a ChRM after 20 mT demagnetization, although some likely have a higher coercivity component that will need to be examined during postexpedition research. APC cores were magnetically oriented and a correction applied to the SRM data for each core.

The first deployment of the subsea camera system was also the inaugural deployment of the newly acquired conductivity, temperature, and depth (CTD) sensor, which was attached to the subsea camera frame. The deployment was successful and produced quality water column data that will aid in identification of water masses.

Site U1558

Background and objectives

Site U1558 (proposed Site SATL-43A) is in the central South Atlantic Ocean, ~1067 km west of the MAR. The objective for Expedition 390C was to core one hole with the APC/XCB system to basement for gas safety monitoring and to install a reentry system with casing through the sediment to ~5 m above basement in a second hole to expedite basement drilling during SAT Expeditions 390 and 393.

Site U1558 is located on Seismic Line CREST1B/C at CDP 3252 near the CREST04 crossing line. A reflector at ~5.9 s TWT was interpreted to be the top of basement and estimated to be at 148 mbsf (Figure **F4**). Basement is predicted to be 49.2 Ma and was formed at

a half spreading rate of ~19.5 mm/y. Oceanic crust at this site is the second oldest crust that will be drilled as part of the SAT expeditions, and it will be compared to older and younger crustal material recovered along the transect. Overlying sediment from Site U1558 is expected to be primarily carbonate ooze, and it will be used in paleoceanographic and microbiological studies.

Operations

Hole U1558A

The *JOIDES Resolution* arrived at Site U1558 on 12 November 2020 after a 92 nmi transit from Site U1557 at an average speed of 11.7 kt and switched to DP mode at 1724 h. No acoustic beacon was deployed. The drill string with the APC/XCB BHA and a nonmagnetic drill collar was lowered, and the bit was spaced out to 4326.7 mbsl based on the precision depth recorder seafloor depth of 4331.6 mbsl. The first mudline core attempted came back empty. The bit was lowered 4 m, and the core was reshot. Hole U1558A was spudded at 0700 h on 13 November and recovered 3.46 m, which established a water depth of 4336.8 m. APC Cores 390C-U1558A-1H through 11H advanced to 94.9 mbsf and recovered 87.87 m (92%). Core 2H experienced low recovery, as at Sites U1556 and U1557, suggesting that there are also one or more hard layers in surface sediment at this site. Core 9H was a partial stroke, advancing only 6 m. Core 10H experienced a strong overpull (70 klb) and was drilled over to release it from the formation. However, because Core 10H was a full stroke, the decision was made to attempt another APC core. Core 11H was a full stroke, but it also experienced a strong overpull and had to be drilled over. The decision was made to switch to the XCB system with the PDC cutting shoe. Cores 1H–11H were oriented with the Icefield MI-5 core orientation tool using a nonmagnetic core barrel following new procedures to identify any rotation relative to the core barrel during deployment. Formation temperatures were measured using the APCT-3 tool on Cores 4H, 7H, and 10H.

XCB Cores 390C-U1558A-12X through 19X advanced from 94.9 to 163.9 mbsf and recovered 50.82 m (74%). Core 12X had a broken liner and was pumped out of the core barrel. A hard layer was encountered at 158.9 mbsf in Core 18X and is tentatively interpreted as the top of basement. Core 18X advanced 2.6 m into the hard layer but recovered almost none of it, aside from ~10 cm of material in the core catcher. Core 19X advanced an additional 2.4 m and recovered 2.62 m of basalt (109%), making overall recovery of hard rock material 52% (Figure **F6**). After Core 19X, we began pulling the drill string back to the surface to prepare for casing and reentry system installation at this site. The bit cleared the rig floor at 0710 h on 15 November, ending Hole U1558A. The XCB PDC cutting shoe was examined and found to be in good condition, again performing exceptionally well in altered basalt material. Overall, coring in Hole U1558A recovered 138.69 m out of the 163.9 m advance (85%) and took 2.6 days of operational time (Table **T2**; Figure **F7**).

Hole U1558B

The ship was offset 20 m east, and preparations for casing and reentry system installation began. The Dril-Quip running tool stand was made up, and the UGH was removed. A casing string of 13⅜ inch casing was made up, followed by a crossover and the 16 inch casing hanger needed to latch in to the reentry system. The first three joints were locked and welded. Sea conditions were unfavorable, and one of the joints was cross threaded during assembly and had to be removed from the string. A replacement casing joint was added, which shortened the casing string slightly to 159.3 m. The plan was for the casing to extend slightly into basement and allow for a second 10¾ inch casing string to be added in the future. We paused operations to wait on weather at 2300 h on 15 November. The reentry cone was lifted off the moonpool doors, and the area was secured for rough seas. Operations resumed at ~0630 h on 16 November 2020. The casing string was lowered and landed in the reentry cone in the moonpool. The bit, mud motor, and underreamer were made up with the underreamer arms set to open to a diameter of 15½ inches. We conducted a test to determine the pump rate required to open the arms of the underreamer (40 strokes/min and 400 lb/inch^2). The rest of the stinger BHA was made up with the Dril-Quip running tool on top. The running tool was latched into the reentry cone, and the driller lifted the complete assembly to measure the weight of the system and check the engagement of the running tool. Finally, the moonpool doors were opened, and the reentry system was lowered through the splash zone at 1220 h. Drill pipe was tripped to the seafloor, pausing to fill pipe with water every ten stands to ensure equalized pressure.

Hole U1558B was spudded at 0120 h on 17 November, and the process of drilling in the reentry cone and 13⅜ inch casing began. The subsea camera system was deployed after the drill-in process began so that the amount of time that the camera was at depth would be limited and a pressure-related failure like the one that occurred at Site U1557 could be avoided. The camera system with the CTD sensor strapped to the frame was deployed through the moonpool at 0700 h and was lowered rapidly toward the seafloor. At 0830 h and a depth of ~3700 mbsl, the video feed failed first on the entry camera and then on the survey camera. The camera system was brought back up to 300 mbsl and kept there so that drilling in the casing could continue without interruption. At 155.9 mbsf, the rate of penetration decreased substantially, indicating that we were now drilling into hard rock material. Basement at Hole U1558B was encountered 3 m shallower than expected based on Hole U1558A (158.9 mbsf). The shallower basement required a longer drilling time than anticipated. We progressed at a rate of ~1 m/h until 1415 h and 161.1 mbsf, when an increase in the measured weight on bit indicated that the reentry cone had landed on the seafloor.

We then spent several hours trying to disconnect the drill string from the reentry system, applying torque to the drill string and attempting to rotate the Dril-Quip running tool 3.5 turns. At 1600 h on 17 November, we were still unable to disengage the running tool and decided to bring the camera back on deck to conduct emergency repairs. While the camera system was being repaired, we continued to attempt to disconnect from the reentry cone without being able to observe it. The ship was moved in a 50 m grid pattern and then a 100 m grid pattern in an attempt to find a position and angle that might allow the tool to release from the reentry cone.

The issue with the subsea camera system was determined to be with the connector between the junction box and telemetry pod, as was the case with the two previous failures. With no remaining spare connectors and with clear evidence that the connectors cannot handle pressure, an alternative solution was found. New fiber and power connections were independently terminated at the junction box and telemetry pod. This solution reduced functionality but provided light and a single video feed. The camera repairs were completed just before midnight on 17 November, and the repaired camera system was deployed through the moonpool at ~0010 h on 18 November. It was lowered rapidly to the seafloor without incident and allowed us to view the reentry cone and drill string, although the Dril-Quip running tool itself was obscured by

suspended sediment and cuttings. Even with the assistance of the camera, we were unable to disconnect the running tool. It appeared that torque applied to the drill string caused rotation of the entire reentry system and mudskirt, not just the running tool. At 0230 h, after a total of 12 h trying to disengage from the reentry system, we made the decision to pull the entire drill string back to the surface, diagnose the issue, and attempt to drill in the casing again in Hole U1558C. The subsea camera was recovered and secured at 0500 h. The next ~12 h were spent tripping pipe back to the surface.

The reentry system was pulled up through the splash zone at 1600 h on 18 November and set onto the moonpool doors. We observed that the Dril-Quip running tool was not easily able to move along the length of the slots to achieve the neutral position required to disengage it. Nonetheless, we were able to rotate and disengage the tool. The tool was lifted to the rig floor and examined. Once on the rig floor, it was able to move freely, and there was nothing obviously wrong with it. The underreamer and bit were also examined and found to be in good condition. The bit cleared the rig floor at 2000 h on 18 November, ending Hole U1558B. Operations in Hole U1558B took 3.5 days of operational time.

Hole U1558C

The Dril-Quip running tool was exchanged for a spare, newly inspected and overhauled one, and the process of redeploying the reentry system began. We again tested the mud motor and underreamer to confirm the pump rate required for rotation and to open the underreamer arms. The stinger was then reassembled, removing a 1 m drill collar pup joint from the original assembly to decrease the distance between the bit and the casing and reduce drilling time in basement. The ship was moved back toward Hole U1558A instead of following the standard offset pattern; we expected that we would encounter hard rock at ~158.9 mbsf instead of the shallower 155.9 mbsf basement depth found in Hole U1558B and thus spend less time drilling in hard rock. The stinger with the mud motor, underreamer, and bit was lowered through the reentry cone and casing, and the running tool at the top of the stinger engaged with the reentry cone. We then opened the moonpool doors, and the reentry cone was lowered through the splash zone at 0245 h on 19 November 2020. We tripped pipe down to the seafloor, filling the drill pipe with water every ten stands. When the bit was near the seafloor, we paused operations to perform a routine slip and cut of the drilling line. We then picked up the top drive and spudded Hole U1558C at 1635 h.

Drilling in the casing continued smoothly through the sediment column. We contacted hard rock at 158.9 mbsf. The subsea camera was deployed just before contact with basement at 0100 h so we could observe the release of the Dril-Quip running tool from the reentry system. Drilling continued until a decrease in hook load indicated that the reentry cone had landed on the seafloor. We slowly transferred the weight of the reentry system with casing to the seafloor while trying to maintain weight on bit. We reached a final hole depth of 162.7 mbsf where we expected that the weight of the reentry system was entirely supported by the seafloor. The next 12 h were spent attempting to disconnect the running tool from the reentry system. As with the Hole U1558B attempt, the ship was moved in a grid pattern to find a position and angle that might allow the tool to release from the reentry cone. We also stopped circulation of drill fluids for several hours so that the formation might collapse around the casing and take the weight of the casing string. We were ultimately unable to disconnect, despite the installation modifications we had made after the first failed attempt. At 1700 h on 20 November, in consultation with the Expedition 390 and 393 Co-Chief Scientists, we made the decision to abandon Hole U1558C and pull the reentry system back to the surface. The subsea camera was recovered at 1800 h, and the process of tripping drill pipe back to the surface began. The bit cleared the seafloor at 1850 h.

The reentry system was raised to just below the ship at ~0600 h on 21 November. We opened the moonpool doors but had zero visibility in the dark and were unable to determine the orientation of the reentry cone base. We paused operations until daylight, when we could safely recover the reentry system. At 0800 h we reopened the moonpool doors, oriented the base, and recovered the reentry system. We observed that three out of four load-bearing plates on the mudskirt had fallen off during the attempted redeployment. As with our first attempt at Hole U1558B, the Dril-Quip running tool was easily disconnected from the reentry system once at the surface despite our inability to disconnect it while on the seafloor. The running tool, underreamer, and bit were raised to the rig floor and inspected. The underreamer was found to be in excellent condition. The bit cleared the rotary table at 1056 h on 21 November, ending Hole U1558C. Operations at Hole U1558C took 2.6 days of operational time.

Hole U1558D

After two failed attempts to install casing and a reentry system at Site U1558, we determined that our inability to disengage the Dril-Quip running tool from the reentry system when on the seafloor was due to hard rock inhibiting the complete transfer of weight off of the tool. The assembly from where the bit sits in hard rock to the running tool is too rigid. As such, the only option for installing a casing and reentry system at Site U1558 was to remove a joint of casing so that the casing shoe landed in sediment above the hard rock contact. We decided to make a final attempt to install this shorter casing string and reentry system. The 16 inch casing hanger was released at 1320 h on 21 November 2020 by screwing releasing bolts into the snap ring that holds the hanger in place in the reentry cone after some initial difficulty compressing the snap ring caused by debris caught in the ring. The hanger was raised to the rig floor and swapped out for a spare. We shortened the casing string by removing a single joint and had reassembled it with a length of 146.1 m by 1745 h (Figure **F9**). The running tool was then latched into the casing hanger, and the hanger landed in the reentry cone. We picked up the mud motor, underreamer, and bit and tested them to determine the pump rates required for rotation and for the underreamer arms to open up. Finally, the casing stinger was lowered to 150 mbrf and the running tool engaged with the reentry cone. New plates were welded onto the mudskirt to replace the ones that were lost.

We opened the moonpool doors and started to lower the reentry cone through the splash zone at ~0245 h on 22 November. On the first attempt, the reentry cone and base slipped out of the bottom snap ring groove, catching on the upper one. We recovered the system, reset the casing hanger snap ring, and attempted a second deployment with the same result. After recovering the system and resetting the snap ring again, we decided to proceed with the deployment. Changing out the reentry system at this stage would require breaking down and then remaking all of the casing, using up the remainder of our operational time. The reentry cone was lowered through the splash zone at 0335 h, and we began the process of tripping drill pipe toward seafloor. Drill pipe was filled with water every ten stands. We closely monitored the weight of the drill string as an indicator of whether the reentry cone was still attached. How-

ever, ship heave generated noisy hook load data that made it difficult to track weight changes on the order of the reentry cone (8.8 klb). At 0600 h, the vessel was moved into position over our proposed location for Hole U1558D (30 m east of Hole U1558A, near Hole U1558B). Prior to the move, the vessel was in an offset position 40 m west and 20 m south of Hole U1558A.

The subsea camera system was deployed at 1200 h on 22 November and lowered toward the seafloor. When the camera caught up with the running tool at 3957.6 mbsl, we observed that the reentry cone had slipped and fallen off of the casing, which was still attached to the drill string via the running tool. We initiated a search for the reentry cone on the seafloor. If it could be located and had landed in proper orientation, we would be able to reenter and drill in the casing as planned. We pulled the subsea camera system back to the surface so that we could remove the drill pipe insert and install a door that enlarges the opening of the camera frame. The camera was redeployed at 1545 h and lowered over the running tool to the bottom of the casing string, just above seafloor. Visibility was good despite the fact that the repaired camera system only has a single functional camera and light. We searched for the reentry cone by moving the ship in an expanding grid pattern, starting at the offset position 40 m west and 20 m south of Hole U1558A. Our best estimate from the hook load data was that the reentry cone had fallen off early in the tripping process, before the ship was positioned over the intended location of Hole U1558D. Ultimately, however, we located the reentry cone and mudskirt at 2223 h, sitting upright on the seafloor in the vicinity of Holes U1558A–U1558C and near its intended position. This location implies that the reentry cone fell off after the ship had moved. We picked up the top drive and prepared to spud Hole U1558D.

The cone was reentered at 0056 h on 23 November, and Hole U1558D was spudded at 0059 h. The drill-in process proceeded smoothly, and the bit achieved a maximum depth of 150.0 mbsf at 0745 h. The length of the shortened casing string was 146.1 m. Basement was estimated to be at ~155.9 mbsf in Hole U1558D. After landing the casing hanger in the reentry system, the Dril-Quip running tool rotated easily and disengaged from the casing and reentry cone at 0750 h. We began pulling the subsea camera and drill string back to the surface and recovered the camera at 0945 h. For the next ~8 h, we pulled the remaining drill pipe to the surface. The running tool was recovered at 1800 h, and the rest of the BHA was pulled up to the rig floor and laid out. The UGH was reinstalled, and the rig floor was secured for transit to Site U1559 at 2356 h, ending Hole U1558D. The vessel switched out of DP mode at 0003 h and was underway at full speed by 0018 h. Operations at Hole U1558D took 2.5 days of operational time.

Principal results

Basement at Site U1558 was determined to be only slightly deeper than estimated from seismic data: at 158.9 mbsf in Holes U1558A and U1558C and at 155.9 mbsf in Hole U1558B, relative to the estimated 148 mbsf. Video footage acquired from the subsea camera during the survey for the reentry cone at Hole U1558D indicates that Holes U1558A and U1558C are <10 m apart, suggesting that there is substantial basement topography within short lateral distances. Figure **F10** compares the geographic coordinates of the Site U1558 holes, taken from the ship at the surface, with where the holes actually appear to be in footage from the subsea camera system. The deep water and long drill string results in the location of the hole not being directly underneath the ship.

Cores 390C-U1558A-1H through 18X were measured on the WR and split-core track systems. Core 19X sections, which contain hard rock material, were measured on the WR tracks but were not split. They were instead preserved in nitrogen gas–flushed bags for description and analysis during Expeditions 390 and 393. The sediment/basement interface occurs in the Core 18X core catcher, which was accidentally split before we realized that the interface was present in that section. The core catcher section halves were subsequently vacuum sealed and stored in D tubes. Core catcher samples from Cores 1H–17X were collected for postexpedition biostratigraphic dating. In addition, we collected one sample per core for headspace gas analysis as well as one to two WR samples per core for chemical analysis of IW. Starting with Core 16X, we collected 10 cm instead of 5 cm WR samples to ensure enough water was available for standard analyses. No systematic core description took place during Expedition 390C. Sediment lithology consists primarily of carbonate ooze, aside from the first two cores. Core 1H is predominantly clay and has a calcium carbonate content of 24.1 wt%. Core 2H contains alternating 0.5–1 m thick clay- and carbonate-rich layers and has a calcium carbonate content of 47.1 wt% at 7.825 mbsf. Below that depth, calcium carbonate content averages 80.1 wt%. Physical properties such as magnetic susceptibility and counts of NGR generally correlate with lithology, with higher magnetic susceptibility values and NGR counts in the clay layers and in the hard rock sections. *P*-wave velocity and GRA density increase downhole, with a significant increase in GRA density values in basement of Core 19X. *P*-wave velocity was not measured in that core.

Data acquired from analysis of IW in Hole U1558A do not show downhole trends as clear as those observed at Sites U1556 and U1557. Alkalinity shows a very narrow range in concentration (2.28–2.56 mM), and concentrations are generally lower than those found at Sites U1556 and U1557. Total dissolved sulfur concentrations, as measured using ICP-AES of IW samples, are relatively constant throughout the sediment column. A maximum concentration of 29.3 mM occurs in the mudline sample, and downhole concentrations average 27.9 ± 0.9 mM. Dissolved manganese (Mn) concentrations increase downhole, reaching a maximum value of 3.02 μM at ~126 mbsf and then decreasing toward basement. Mn concentrations are significantly lower than at Sites U1556 and U1557, where peak Mn concentrations are >100 μM. The peak in dissolved Mn at ~126 mbsf is followed by a sharp peak in ammonium (reaching 213.4 μM at ~130 mbsf) and then a sharp decline in sulfur to a minimum of 24.5 mM at ~137 mbsf. These respective maximum and minimum values are only present in one or two samples and will need to be confirmed through higher resolution sampling during Expeditions 390 and 393. Combined, however, the data suggest a deep redox horizon and indicate that the upper sediment column may be oxygenated. This hypothesis can be verified with direct measurements of dissolved oxygen during Expeditions 390 and 393. Dissolved iron was below the detection limit, likely because it reoxidized and precipitated during the WR squeezing process.

Dissolved calcium and strontium concentrations increase downhole before decreasing again just above basement; the inflection point is ~140 m. Their concentrations in IW are overall lower than at Sites U1556 and U1557. Conversely, dissolved magnesium and potassium concentrations decrease slightly with depth and do not show a near-basement reversal in the trend. Dissolved silicon concentrations decrease from the surface to ~25 mbsf and then remain relatively constant with depth. Boron concentrations decrease initially but increase again at ~115 mbsf. The two elements do not

have the close inverse correlation observed at Sites U1556 and U1557.

All cores excluding the unsplit basement sections were measured on the SRM for NRM and then at alternating field demagnetization levels of 5, 10, and 20 mT. Vertical drilling overprints were ubiquitous but were generally removed by the 5 mT demagnetization step. Many samples appeared to show a ChRM after 20 mT demagnetization, although some likely have a higher coercivity component that will need to be examined during postexpedition research.

The CTD sensor was deployed along with the subsea camera system at Hole U1558B. It successfully logged water column data.

Site U1559

Site U1559 (proposed site SATL-13A) is in the central South Atlantic Ocean, ~130 km west of the MAR. The objective for Expedition 390C was to core one hole with the APC/XCB system to basement for gas safety monitoring and to install a reentry system with casing through the sediment to ~5 m above basement in a second hole to expedite basement drilling during SAT Expeditions 390 and 393.

Site U1559 is located on Seismic Line CREST01 at CDP 11923 between the CREST06 and CREST1E/F crossing lines. A reflector at ~4.15 s TWT is interpreted to be the top of basement and was estimated at 50 mbsf (Figure **F4**). Basement is predicted to be approximately 6.6 Ma and formed at a half spreading rate of ~17.0 mm/y. This site was selected as the young crustal end-member of the SAT and will be compared to older crustal material cored at sites further west. The site is similar in age to Hole 504B in the eastern equatorial Pacific (6.9 Ma), which formed at an intermediate rate (36 mm/y half spreading rate) and is covered by 275 m of sediment. As such, material from Site U1559 will allow comparison of how alteration progresses at different spreading centers and with different thicknesses of overlying sediment and sedimentation histories. Overlying sediment from Site U1559 is expected to be primarily carbonate ooze and will be used in paleoceanographic and microbiological studies.

Operations

Hole U1559A

The *JOIDES Resolution* completed the 508 nmi transit to Site U1559 from Site U1558 at an average speed of 12.3 kt. We arrived on site at 1715 h on 25 November 2020, lowered the thrusters, and were in DP mode ready to begin operations by 1740 h. An acoustic beacon was not deployed. The APC/XCB BHA with a nonmagnetic drill collar was made up and deployed, and we began tripping pipe toward the seafloor. Hole U1559A was spudded at 0140 h on 26 November with the bit positioned at 3049.7 mbsl, and Core 390C-U1559A-1H recovered 3.54 m of sediment. The mudline core established the water depth as 3055.7 mbsl. APC coring continued through Core 4H, advancing to 32 mbsf and recovering 32.9 m of sediment (103%). After Core 4H, we transitioned to the XCB coring system because basement was estimated to be at 50 mbsf. No magnetic orientation or temperature measurements were conducted with the APC cores because of time constraints and because we did not want to damage tools if we encountered basement at a shallower depth than expected. XCB Cores 5X–8X advanced from 32 to 64.7 mbsf. We encountered a hard layer at 64.0 mbsf that dramatically decreased the rate of penetration to <1 m/h. Recovery of this layer was poor: ~11% of the 0.7 m advance and ~8 cm of small, rubbly pieces of basalt. The XCB PDC cutting shoe lost several cutters while coring Core 8X. It is unclear whether the lost cutters were due to cumulative use during the entire expedition or difficulty in cutting this younger basalt material. Core 9X was drilled by time (140 min) rather than by advance because the penetration rate was extremely low and we wanted to avoid damaging the bit by exposing it to elevated temperatures. Ultimately, Core 9X advanced 1.5 m at a rate of 0.64 m/h. Only 0.39 m of material was recovered (26%), consisting of indurated sediment and altered glass (Figure **F6**). Excluding hard rock material, Cores 5X–8X advanced 32 m and recovered 24.64 m (77%). In total, Hole U1559A penetrated to 66.2 mbsf with a recovery of 58.01 m (88%) (Table **T2**; Figure **F7**). We began pulling out of the hole after Core 9X to have time to install a reentry system with casing. The bit cleared the rig floor at 2200 h, ending Hole U1559A. Overall, coring in Hole U1559A took 1.2 days of operational time.

Hole U1559B

To prepare for installation of the reentry system at Hole U1559B, the UGH was removed and the reentry cone was positioned above the moonpool doors underneath the rig floor. The casing shoe was found to be damaged, and a new one was prepared. Four joints of 13⅜ inch casing were made up, followed by a crossover and the 16 inch casing hanger needed to latch into the reentry cone. One joint of casing was found to have a bent coupling and was replaced. Once the casing string was made up, the Dril-Quip running tool was used to lower it through the reentry cone and latch it into place. Next, the BHA with the bit, underreamer, and mud motor was made up and lowered through the casing, and the running tool engaged with the reentry system. The moonpool doors were opened, and the reentry system was lowered through the splash zone at 1645 h on 27 November 2020. The reentry system was lowered at a controlled rate of descent, pausing to fill the drill pipe with water every 10 stands to ensure equalized pressure. The subsea camera was deployed at 2345 h to observe the casing drill-in process and release. The CTD sensor was attached to the frame of the subsea camera system and logged water column data during the camera deployment.

With the bit spaced out to 3022.7 mbsl, we picked up the top drive and spudded Hole U1559B at 0130 h on 28 November, establishing the seafloor depth as 3055.0 m. The bit reached its maximum depth of 58.9 mbsf by 0315 h with the casing shoe at 55.3 mbsf (Figure **F11**). Basement is expected to be at 64.0 mbsf. With the reentry system on the seafloor, the driller then applied torque to rotate the running tool 3.5 times, releasing it from the reentry system and casing. We pulled out of the hole, and the bit cleared the reentry cone at 0358 h. The subsea camera was pulled back to the surface and recovered at 0415 h. The top drive was set back, and fluid was circulated through the drill string, displacing seawater with freshwater in the drill pipe. We tripped the rest of the drill pipe back to surface, recovered and laid out the BHA, and detorqued the running tool. The UGH was reinstalled, and the moonpool was secured. The rig floor was secured for transit at 1815 h, ending Hole U1559B as well as operations for Expedition 390C. Overall, Hole U1559B took 1.8 days of operational time. The ship transitioned out of DP mode and got underway. The 1723 nmi transit to Cape Town, South Africa, was anticipated to take ~6.5 days with an estimated arrival on 5 December.

Principal results

Basement at Site U1559 was determined to be only slightly deeper than estimated from seismic data: at 64.0 mbsf relative to the

estimated 50 mbsf. Cores 390C-U1559A-1H through 7X were measured on the WR and split-core track systems. Sections from Cores 8X and 9X, which contain hard rock material, were measured on the WR tracks but were not split. They were instead preserved in nitrogen gas–flushed bags for description and analysis during Expeditions 390 and 393. Core catcher samples from Cores 1H–7X were collected for postexpedition biostratigraphic dating. In addition, we collected one sample per core for headspace gas analysis as well as one to two WR samples per core for chemical analysis of IW. No systematic core description took place during Expedition 390C. Sediment lithology consists of carbonate ooze. Sediment color is slightly darker in the first core and then transitions to a lighter white throughout the rest of the hole. However, even in this upper, darker core, calcium carbonate content is 92.2 wt%. Physical properties generally correlate with lithology. Counts of NGR peak in the first section of the first core, decline rapidly through the first core, and then continue to decrease slowly with depth throughout the hole.

Data acquired from analysis of IW in Hole U1559A do not show downhole trends as clear as those observed at Sites U1556 and U1557. Alkalinity is relatively low in the mudline sample (2.32 mM), increases to a broad maximum at ~30 mbsf, and then decreases again toward basement. Similar to results from Hole U1558A, the range in alkalinity concentrations (2.24–2.90 mM) is less than that found at Sites U1556 and U1557. Total dissolved sulfur concentrations, as measured using ICP-AES of IW samples, likewise do not vary substantially downhole, ranging from 29.6 mM in the mudline sample to a minimum of 28.2 mM at 60.175 mbsf. Total sulfur concentrations are similar in value to sulfate concentrations measured by ion chromatography. There is no indication of significant sulfate reduction in the sediment column at this site. Dissolved Mn concentrations do show a subsurface maximum, however, suggesting reduction of oxidized Mn mineral phases. Dissolved iron is below the detection limit, likely because it reoxidized and precipitated during the WR squeezing process. There is no clear trend in ammonium concentrations, which were near the detection limit of the spectrophotometer.

Dissolved calcium (Ca) data do not show a clear trend in the top portion of the hole, although concentrations reach maximum values between ~20 and 40 mbsf and then decrease again toward basement. Strontium (Sr) concentrations more clearly increase to this depth and then decrease toward basement. As with data from Hole U1558A, Ca and Sr concentrations are lower than at Sites U1556 and U1557. Dissolved magnesium concentrations are variable with depth, whereas potassium increases slightly with a sharp decrease just above the hard rock contact at 64.0 mbsf. Dissolved silicon concentrations are low in the mudline sample, relatively constant with depth, and then increase above basement. Boron concentrations are low in the mudline sample, increase with depth, and then decrease slightly above basement.

All cores excluding the unsplit basement sections were measured on the SRM for NRM and then at alternating field demagnetization levels of 5, 10, and 20 mT. Vertical drilling overprints were ubiquitous but were generally removed by the 5 mT demagnetization step. Many samples appeared to show a ChRM after 20 mT demagnetization, although some likely have a higher coercivity component that will need to be examined during postexpedition research. A spike in intensity at the top of Section 390C-U1559A-7X-1 was likely caused by a small piece of hard material, possibly basalt, which is observable in the X-ray images.

The CTD sensor was deployed along with the subsea camera system at Hole U1559B. It successfully logged water column data.

Preliminary scientific assessment

The primary goal of Expedition 390C was to complete casing and reentry system installations in advance of Expeditions 390 and 393. Secondary goals included coring across the sediment/basement interface with the XCB coring system and analyzing cored material for ephemeral properties. The operational plan evolved over the course of the expedition, first growing in scope to include work at Sites U1556 and U1557 when the end port for the expedition was changed to Cape Town, South Africa, from Las Palmas, Canary Islands (Spain), and then decreasing in scope as reentry system installations did not proceed smoothly. With transits from Kristiansand, Norway, to Cape Town, Expedition 390C had 32 days of operational time along the SAT (Figures **F12**, **F13**). Figure **F14** shows work completed at SAT sites in addition to the remaining operational objectives to be accomplished during future SAT expeditions.

Operational considerations

In an effort to facilitate the long-term goal of installing borehole observatories at SAT sites, we attempted to install casing into basement at Site U1558. Both attempts (Holes U1558B and U1558C) resulted in our being unable to disengage the Dril-Quip running tool from the casing hanger and necessitated pulling the entire drill string, including the reentry system and casing, back to the surface. We hypothesize that the rigidity of the BHA between the running tool and the drill bit in hard rock prevents the complete transfer of weight off of the running tool, which in turn inhibits our ability to move the running tool into the neutral position so that it can be rotated and released. In both instances, the running tool was easily disengaged at the surface. When the casing shoe was positioned in sediment in Holes U1557D, U1558D, and U1559B, the tool was also easily disengaged. This outcome suggests that, for future endeavors involving installation of casing into basement, either a hydraulic release tool (HRT) reentry system should be used or the hole should be fully drilled out beyond the intended depth of the casing shoe prior to casing installation.

At all sites, the XCB system with a PDC cutting shoe was used to advance 2–10 m into hard rock material with the goal of capturing the sediment/basement interface. Although not designed for drilling in hard rock material, the cutting shoe performed extremely well, particularly in the altered basalts and indurated sediment encountered at Sites U1556–U1558. We experienced relatively high recoveries (>50% of cored hard rock material at those sites) and recovered large, well-trimmed pieces with comparatively few "rollers" (small pieces of rock that may have shifted in position and orientation during recovery). In Hole U1559A, our time was limited and we were only able to advance ~2 m into basement, experiencing poor recovery. Recovered hard rock consisted of small, rubbly pieces of basalt and indurated sediment. Four of six cutters from the PDC cutting shoe were lost while drilling Core 390C-U1559-8X. Core 9X, deployed with the alternate PDC cutting shoe, did not recover any of the cutters lost during Core 8X and did not lose cutters, although two were chipped.

It is unclear whether the damage to the PDC cutting shoes in Cores 390C-U1559-8X and 9X can be attributed to cumulative wear over the course of the expedition or difficulty in drilling younger basalt material. In either case, the PDC cutting shoe outperformed the tungsten carbide insert (TCI) cutting shoes that have been used previously in similar environments. This result may be due to the different cutting shoe material (PDC rather than tungsten carbide) or

may be attributable to the design and geometry of the shoe. The TCI cutting shoes have one fewer cutter and fewer jets, reducing fluid circulation and cooling capability. In addition, the TCI cutters are all oriented inwards, whereas the PDC cutting shoe has three cutters oriented inward and three oriented outward, more completely separating the core from the formation. Because capturing the sediment/basement interface is often a science priority, the positive results from this expedition merit further investigation.

Preliminary assessment of scientific objectives

At Site U1556, the hard rock contact was significantly deeper than estimated (at 278 mbsf instead of the estimated 180 mbsf); a shallow reflection at 6.9 s TWT that marked a change in seismic character from high-frequency to low-frequency reflectivity was misinterpreted to be basement. A deeper reflector has been reinterpreted to be basement. Further coring and logging operations will provide insight into what generates the observed reflectors (Figure **F4**). The thick sediment layer at Site U1556 and consequent reinterpretation of seismic data also led us to designate proposed Site SATL-56A a primary site instead of proposed Site SATL-54A, which had an estimated basement contact at 639 mbsf. At that depth, or any deeper, we would not be able to install casing all the way to basement because of concerns about drill string weight that limit the maximum deployable casing string length to ~600 m in that water depth (~5000 mbsl). The hard rock contact was slightly deeper than estimated at all other sites, likely because of slight differences in seismic velocities from what was expected.

XCB coring advanced between 2 and 10 m into hard rock material at all Expedition 390C sites. At most sites, however, the hard rock was not true basalt basement but a mixture of indurated sediment, volcaniclastics, and basalt (Figure **F6**). Material recovered from Site U1558 appears to be true basalt crust, although drilling has advanced only 5 m. For all sites, it remains undetermined how thick this layer of transition material is.

Lithology of recovered sediment was as expected: primarily carbonate ooze, with occasional clay layers. Systematic core description will occur during Expeditions 390 and 393. Sediment from the westernmost Sites, U1556 and U1557, records alternations between carbonate-rich and carbonate-poor sediment that are possibly related to fluctuations in the depth of the CCD, a science objective for the expeditions. IW chemical data also indicate that Expedition 390 and 393 sites will provide the necessary material to address the science objectives. Increased concentrations of dissolved magnesium and potassium in WR samples from just above the sediment/basement interface at Sites U1556 and U1557 suggest fluid flow along or near the interface. Clearly defined redox horizons at Sites U1556 and U1557 (apparent in the manganese, ammonium, and sulfur data) will guide microbiological sampling efforts during Expeditions 390 and 393, particular those targeting sulfur metabolisms. At Sites U1558 and U1559, the pore water data show less pronounced depth trends, but the relatively low concentrations of dissolved manganese and ammonium as well as the high concentrations of sulfur suggest deep penetration of oxygen into the sediment column.

Outreach

No Onboard Outreach Officer sailed during Expedition 390C. Limited social media posts were made via the *JOIDES Resolution* Facebook and Twitter accounts. Table **T3** summarizes social media interactions.

References

Alt, J.C., and Teagle, D.A.H., 1999. The uptake of carbon during alteration of ocean crust. *Geochimica et Cosmochimica Acta*, 63(10):1527–1535. **https://doi.org/10.1016/S0016-7037(99)00123-4**

Anderson, R.N., Honnorez, J., Becker, K., and et al., 1985. *Initial Reports of the Deep Sea Drilling Project*, 83: Washington, DC (U.S. Government Printing Office). **https://doi.org/10.2973/dsdp.proc.83.1985**

Bach, W., and Edwards, K.J., 2003. Iron and sulfide oxidation within the basaltic ocean crust: implications for chemolithoautotrophic microbial biomass production. *Geochimica et Cosmochimica Acta*, 67(20):3871–3887. **https://doi.org/10.1016/S0016-7037(03)00304-1**

Barker, P.F., and Thomas, E., 2004. Origin, signature and palaeoclimatic influence of the Antarctic Circumpolar Current. *Earth-Science Reviews*, 66(1–2):143–162. **https://doi.org/10.1016/j.earscirev.2003.10.003**

Barrera, E., Savin, S.M., Thomas, E., and Jones, C.E., 1997. Evidence for thermohaline-circulation reversals controlled by sea-level change in the latest Cretaceous. *Geology*, 25(8):715–718. **https://doi.org/10.1130/0091-7613(1997)025%3C0715:EFTCRC%3E2.3.CO;2**

Berner, R.A., Lasaga, A.C., and Garrels, R.M., 1983. The carbonate-silicate geochemical cycle and its effect on atmospheric carbon dioxide over the past 100 million years. *American Journal of Science*, 283(7):641–683. **https://doi.org/10.2475/ajs.283.7.641**

Billups, K., 2002. Late Miocene through early Pliocene deep water circulation and climate change viewed from the sub-Antarctic South Atlantic. *Palaeogeography, Palaeoclimatology, Palaeoecology*, 185(3):287–307. **https://doi.org/10.1016/S0031-0182(02)00340-1**

Bohaty, S.M., Zachos, J.C., Florindo, F., and Delaney, M.L., 2009. Coupled greenhouse warming and deep-sea acidification in the middle Eocene. *Paleoceanography and Paleoclimatology*, 24(2):PA2207. **https://doi.org/10.1029/2008PA001676**

Borrelli, C., Cramer, B.S., and Katz, M.E., 2014. Bipolar Atlantic deepwater circulation in the middle-late Eocene: effects of Southern Ocean gateway openings. *Paleoceanography and Paleoclimatology*, 29(4):308–327. **https://doi.org/10.1002/2012PA002444**

Broecker, W.S., 1991. The great ocean conveyor. *Oceanography*, 4(2):79–89. **https://www.jstor.org/stable/43924572**

Cande, S.C., and Kent, D.V., 1995. Revised calibration of the geomagnetic polarity timescale for the Late Cretaceous and Cenozoic. *Journal of Geophysical Research*, 100(B4):6093–6095. **https://doi.org/10.1029/94JB03098**

Coggon, R.M., and Teagle, D.A.H., 2011. Hydrothermal calcium-carbonate veins reveal past ocean chemistry. *TrAC Trends in Analytical Chemistry*, 30(8):1252–1268. **https://doi.org/10.1016/j.trac.2011.02.011**

Coggon, R.M., Teagle, D.A.H., Cooper, M.J., and Vanko, D.A., 2004. Linking basement carbonate vein compositions to porewater geochemistry across the eastern flank of the Juan de Fuca Ridge, ODP Leg 168. *Earth and Planetary Science Letters*, 219(1):111–128. **https://doi.org/10.1016/S0012-821X(03)00697-6**

Coggon, R.M., Teagle, D.A.H., Smith-Duque, C.E., Alt, J.C., and Cooper, M.J., 2010. Reconstructing past seawater Mg/Ca and Sr/Ca from mid-ocean ridge flank calcium carbonate veins. *Science*, 327(5969):1114–1117. **https://doi.org/10.1126/science.1182252**

Cramer, B.S., Toggweiler, J.R., Wright, J.D., Katz, M.E., and Miller, K.G., 2009. Ocean overturning since the Late Cretaceous: inferences from a new benthic foraminiferal isotope compilation. *Paleoceanography and Paleoclimatology*, 24(4):PA4216. **https://doi.org/10.1029/2008PA001683**

Davis, A.C., Bickle, M.J., and Teagle, D.A.H., 2003. Imbalance in the oceanic strontium budget. *Earth and Planetary Science Letters*, 211(1):173–187. **https://doi.org/10.1016/S0012-821X(03)00191-2**

Devey, C., 2014. SoMARTherm: The Mid-Atlantic Ridge 13–33°S - Cruise No. MSM25 - January 24–March 5, 2013 - Cape Town (South Africa) - Mindelo (Cape Verde). DFG Senate Commission for Oceanography. **https://doi.org/10.2312/cr_msm25**

D'Hondt, S., Inagaki, F., Alvarez Zarikian, C., Abrams, L.J., Dubois, N., Engelhardt, T., Evans, H., et al., 2015. Presence of oxygen and aerobic commu-

nities from sea floor to basement in deep-sea sediments. *Nature Geoscience*, 8(4):299–304. **https://doi.org/10.1038/NGEO2387**

Dickens, G.R., Castillo, M.M., and Walker, J.C.G., 1997. A blast of gas in the latest Paleocene: simulating first-order effects of massive dissociation of oceanic methane hydrate. *Geology*, 25(3):259–262. **https://doi.org/10.1130/0091-7613(1997)025%3C0259:ABOGIT%3E2.3.CO;2**

Engelen, B., Ziegelmüller, K., Wolf, L., Köpke, B., Gittel, A., Cypionka, H., Treude, T., et al., 2008. Fluids from the oceanic crust support microbial activities within the deep biosphere. *Geomicrobiology Journal*, 25(1):56–66. **https://doi.org/10.1080/01490450701829006**

Estep, J., Reece, R., Kardell, D.A., Christeson, G.L., and Carlson, R.L., 2019. Seismic Layer 2A: evolution and thickness from 0- to 70-Ma crust in the slow-intermediate spreading South Atlantic. *Journal of Geophysical Research: Solid Earth*, 124(8):7633–7651. **https://doi.org/10.1029/2019JB017302**

Expedition 301 Scientists, 2005. Expedition 301 summary. *In* Fisher, A.T., Urabe, T., Klaus, A., and the Expedition 301 Scientists (Eds.), *Proceedings of the Integrated Ocean Drilling Program,* 301: College Station, TX (Integrated Ocean Drilling Program Management International). **https://doi.org/10.2204/iodp.proc.301.101.2005**

Expedition 309/312 Scientists, 2006. Expedition 309/312 summary. *In* Teagle, D.A.H., Alt, J.C., Umino, S., Miyashita, S., Banerjee, N.R., Wilson, D.S., and the Expedition 309/312 Scientists (Eds.), *Proceedings of the Integrated Ocean Drilling Program,* 309: Washington, DC (Integrated Ocean Drilling Program Management International, Inc.). **https://doi.org/10.2204/iodp.proc.309312.101.2006**

Expedition 327 Scientists, 2011. Expedition 327 summary. *In* Fisher, A.T., Tsuji, T., Petronotis, K., and the Expedition 327 Scientists (Eds.), *Proceedings of the Integrated Ocean Drilling Program,* 327: Tokyo (Integrated Ocean Drilling Program Management International, Inc.). **https://doi.org/10.2204/iodp.proc.327.101.2011**

Expedition 329 Scientists, 2011. Expedition 329 summary. *In* D'Hondt, S., Inagaki, F., Alvarez Zarikian, C.A., and the Expedition 329 Scientists (Eds.), *Proceedings of the Integrated Ocean Drilling Program,* 332: Tokyo (Integrated Ocean Drilling Program Management International, Inc.). **https://doi.org/10.2204/iodp.proc.329.101.2011**

Expedition 329 Scientists, 2012. Expedition 330 summary. *In* D'Hondt, S., Inagaki, F., Alvarez Zarikian, C.A., and the Expedition 329 Scientists (Eds.), *Proceedings of the Integrated Ocean Drilling Program,* 330: Tokyo (Integrated Ocean Drilling Program Management International, Inc.). **https://doi.org/10.2204/iodp.proc.330.101.2012**

Expedition 335 Scientists, 2012. Expedition 335 summary. *In* Teagle, D.A.H., Ildefonse, B., Blum, P., and the Expedition 335 Scientists (Eds.), *Proceedings of the Integrated Ocean Drilling Program,* 335: Tokyo (Integrated Ocean Drilling Program Management International, Inc.). **https://doi.org/10.2204/iodp.proc.335.101.2012**

Expedition 336 Scientists, 2012. Expedition 336 summary. *In* Edwards, K.J., Bach, W., Klaus, A., and the Expedition 336 Scientists (Eds.), *Proceedings of the Integrated Ocean Drilling Program,* 336: Tokyo (Integrated Ocean Drilling Program Management International, Inc.). **https://doi.org/10.2204/iodp.proc.336.101.2012**

Frank, T.D., and Arthur, M.A., 1999. Tectonic forcings of Maastrichtian ocean-climate evolution. *Paleoceanography and Paleoclimatology*, 14(2):103–117. **https://doi.org/10.1029/1998PA900017**

Gillis, K.M., and Coogan, L.A., 2011. Secular variation in carbon uptake into the ocean crust. *Earth and Planetary Science Letters*, 302(3):385–392. **https://doi.org/10.1016/j.epsl.2010.12.030**

Inagaki, F., and Orphan, V., 2014. Exploration of subseafloor life and the biosphere through IODP (2003–2013). *In* Stein, R., Blackman, D.K., Inagaki, F., and Larsen, H.-C. (Eds.), *Developments in Marine Geology* (Volume 7): *A Decade of Science Achieved by the Integrated Ocean Drilling Program (IODP),* 39–63. **https://doi.org/10.1016/B978-0-444-62617-2.00002-5**

Inagaki, F., Nunoura, T., Nakagawa, S., Teske, A., Lever, M., Lauer, A., Suzuki, M., et al., 2006. Biogeographical distribution and diversity of microbes in methane hydrate-bearing deep marine sediments on the Pacific Ocean margin. *Proceedings of the National Academy of Sciences of the United States of America*, 103(8):2815–2820. **https://doi.org/10.1073/pnas.0511033103**

Jungbluth, S.P., Grote, J., Lin, H.-T., Cowen, J.P., and Rappe, M.S., 2013. Microbial diversity within basement fluids of the sediment-buried Juan de Fuca Ridge flank. *The ISME Journal*, 7(1):161–172. **https://doi.org/10.1038/ismej.2012.73**

Kallmeyer, J., Pockalny, R., Adhikari, R.R., Smith, D.C., and D'Hondt, S., 2012. Global distribution of microbial abundance and biomass in subseafloor sediment. *Proceedings of the National Academy of Sciences of the United States of America*, 109(40):16213–16216. **https://doi.org/10.1073/pnas.1203849109**

Kardell, D.A., Christeson, G.L., Estep, J.D., Reece, R.S., and Carlson, R.L., 2019. Long-lasting evolution of Layer 2A in the western South Atlantic: evidence for low-temperature hydrothermal circulation in old oceanic crust. *Journal of Geophysical Research: Solid Earth*, 124(3):2252–2273. **https://doi.org/10.1029/2018JB016925**

Katz, M.E., Cramer, B.S., Toggweiler, J.R., Esmay, G., Liu, C., Miller, K.G., Rosenthal, Y., Wade, B.S., and Wright, J.D., 2011. Impact of Antarctic Circumpolar Current development on late Paleogene ocean structure. *Science*, 332(6033):1076–1079. **https://doi.org/10.1126/science.1202122**

Kennett, J.P., and Stott, L.D., 1990. Proteus and proto-oceanus: ancestral Paleogene oceans as revealed from Antarctic stable isotopic results; ODP Leg 113. *In* Barker, P.F., Kennett, J.P., et al. (Eds.), *Proceedings of the Ocean Drilling Program, Scientific Results,* 113: College Station, TX (Ocean Drilling Program), 865–880. **https://doi.org/10.2973/ODP.PROC.SR.113.188.1990**

Kennett, J.P., and Stott, L.D., 1991. Abrupt deep-sea warming, palaeoceanographic changes and benthic extinctions at the end of the Palaeocene. *Nature*, 353(6341):225–229. **https://doi.org/10.1038/353225a0**

Lee, H.J., Jeong, S.E., Kim, P.J., Madsen, E.L., and Jeon, C.O., 2015. High resolution depth distribution of bacteria, archaea, methanotrophs, and methanogens in the bulk and rhizosphere soils of a flooded rice paddy. *Frontiers in Microbiology*, 6:639. **https://doi.org/10.3389/fmicb.2015.00639**

Lever, M.A., Rogers, K.L., Lloyd, K.G., Overmann, J., Schink, B., Thauer, R.K., Hoehler, T.M., and Jørgensen, B.B., 2015. Life under extreme energy limitation: a synthesis of laboratory- and field-based investigations. *FEMS Microbiology Reviews*, 39(5):688–728. **https://doi.org/10.1093/femsre/fuv020**

Lever, M.A., Rouxel, O., Alt, J.C., Shimizu, N., Ono, S., Coggon, R.M., Shanks, W.C., III, et al., 2013. Evidence for microbial carbon and sulfur cycling in deeply buried ridge flank basalt. *Science*, 339(6125):1305–1308. **https://doi.org/10.1126/science.1229240**

Lomstein, B.A., Langerhuus, A.T., D'Hondt, S., Jørgensen, B.B., and Spivack, A.J., 2012. Endospore abundance, microbial growth and necromass turnover in deep sub-seafloor sediment. *Nature*, 484(7392):101–104. **https://doi.org/10.1038/nature10905**

Mallows, C., and Searle, R.C., 2012. A geophysical study of oceanic core complexes and surrounding terrain, Mid-Atlantic Ridge 13°N–14°N. *Geochemistry, Geophysics, Geosystems*, 13(6):Q0AG08. **https://doi.org/10.1029/2012GC004075**

Mason, O.U., Nakagawa, T., Rosner, M., Van Nostrand, J.D., Zhou, J., Maruyama, A., Fisk, M.R., and Giovannoni, S.J., 2010. First investigation of the microbiology of the deepest layer of ocean crust. *PloS One*, 2010. **https://doi.org/10.1371/journal.pone.0015399**

Maus, S., Barckhausen, U., Berkenbosch, H., Bournas, N., Brozena, J., Childers, V., Dostaler, F., et al., 2009. EMAG2: a 2–arc min resolution Earth Magnetic Anomaly Grid compiled from satellite, airborne, and marine magnetic measurements. *Geochemistry, Geophysics, Geosystems*, 10(8):Q08005. **https://doi.org/10.1029/2009GC002471**

Mottl, M.J., 2003. Partitioning of energy and mass fluxes between mid-ocean axes and flanks at high and low temperature. *In* Halbech, P.E., Tunnicliffe, V., and Hein, J.R. (Eds.), *Energy and Mass Transfer in Marine Hydrothermal Systems:* Berlin (Dahlem University Press), 271–286.

Müller, R.D., Sdrolias, M., Gaina, C., Steinberger, B., and Heine, C., 2008. Long-term sea-level fluctuations driven by ocean basin dynamics. *Science*, 319(5868):1357–1362. **https://doi.org/10.1126/science.1151540**

Norris, R.D., Wilson, P.A., Blum, P., Fehr, A., Agnini, C., Bornemann, A., Boulila, S., Bown, P.R., Cournede, C., Friedrich, O., Ghosh, A.K., Hollis, C.J., Hull, P.M., Jo, K., Junium, C.K., Kaneko, M., Liebrand, D., Lippert, P.C., Zhonghui, L., Matsui, H., Moriya, K., Nishi, H., Opdyke, B.N., Penman, D., Romans, B., Scher, H.D., Sexton, P., Takagi, H., Kirtland Turner, S., Whiteside, J.H., Yamaguchi, T., and Yamamoto, Y., 2014. Expedition 342 summary. *In* Norris, R.D., Wilson, P.A., Blum, P., and the Expedition 342 Scientists (Eds.), *Proceedings of the Integrated Ocean Drilling Program,* 342: College Station, TX (Integrated Ocean Drilling Program). **https://doi.org/10.2204/iodp.proc.342.101.2014**

Orcutt, B.N., Wheat, C.G., Rouxel, O., Hulme, S., Edwards, K.J., and Bach, W., 2013. Oxygen consumption rates in subseafloor basaltic crust derived from a reaction transport model. *Nature Communications*, 4:2539. **https://doi.org/10.1038/ncomms3539**

Orcutt, B.N., Bach, W., Becker, K., Fisher, A.T., Hentscher, M., Toner, B.M., Wheat, C.G., and Edwards, K.J., 2011. Colonization of subsurface microbial observatories deployed in young ocean crust. *The ISME Journal*, 5(4):692–703. **https://doi.org/10.1038/ismej.2010.157**

Orcutt, B.N., LaRowe, D.E., Lloyd, K.G., Mills, H., Orsi, W., Reese, B.K., Sauvage, J., Huber, J.A., and Amend, J., 2014. IODP Deep Biosphere Research Workshop report – a synthesis of recent investigations, and discussion of new research questions and drilling targets. *Scientific Drilling*, 17:61–66. **https://doi.org/10.5194/sd-17-61-2014**

Pälike, H., Lyle, M.W., Nishi, H., Raffi, I., Ridgwell, A., Gamage, K., Klaus, A., et al., 2012. A Cenozoic record of the Equatorial Pacific carbonate compensation depth. *Nature*, 488(7413):609–614. **https://doi.org/10.1038/nature11360**

Palmer, M.R., and Edmond, J.M., 1989. The strontium isotope budget of the modern ocean. *Earth and Planetary Science Letters*, 92(1):11–26. **https://doi.org/10.1016/0012-821X(89)90017-4**

Penrose Conference Participants, 1972. Penrose field conference on ophiolites. *Geotimes*, 17(12):24–25.

Perfit, M.R., and Chadwick, W.W., Jr., 1998. Magmatism at mid-ocean ridges: constraints from volcanological and geochemical investigations. *In* Buck, W.R., Delaney, J.A., Karson, J.A., and Lagabrielle, Y. (Eds.), *Faulting and Magmatism at Mid-Ocean Ridges,* 59–115. **https://doi.org/10.1029/GM106p0059**

Rausch, S., Böhm, F., Bach, W., Klügel, A., and Eisenhauer, A., 2013. Calcium carbonate veins in ocean crust record a threefold increase of seawater Mg/Ca in the past 30 million years. *Earth and Planetary Science Letters*, 362:215–224. **https://doi.org/10.1016/j.epsl.2012.12.005**

Reese, B.K., Zinke, L.A., Sobol, M.S., LaRowe, D.E., Orcutt, B.N., Zhang, X., Jaekel, U., et al., 2018. Nitrogen cycling of active bacteria within oligotrophic sediment of the Mid-Atlantic Ridge flank. *Geomicrobiology Journal*, 35(6):468–483. **https://doi.org/10.1080/01490451.2017.1392649**

Ryan, W.B.F., Carbotte, S.M., Coplan, J.O., O'Hara, S., Melkonian, A., Arko, R., Weissel, R.A., et al., 2009. Global Multi-Resolution Topography synthesis. *Geochemistry, Geophysics, Geosystems*, 10(3):Q03014. **https://doi.org/10.1029/2008GC002332**

Santelli, C.M., Edgcomb, V.P., Bach, W., and Edwards, K.J., 2009. The diversity and abundance of bacteria inhabiting seafloor lavas positively correlate with rock alteration. *Environmental Microbiology*, 11(1):86–98. **https://doi.org/10.1111/j.1462-2920.2008.01743.x**

Scher, H.D., and Martin, E.E., 2006. Timing and climatic consequences of the opening of Drake Passage. *Science*, 312(5772):428–430. **https://doi.org/10.1126/science.1120044**

Schmid, F., Peters, M., Walter, M., Devey, C., Petersen, S., Yeo, I., Köhler, J., Jamieson, J.W., Walker, S., and Sültenfuß, J., 2019. Physico-chemical properties of newly discovered hydrothermal plumes above the southern Mid-Atlantic Ridge (13°–33°S). *Deep Sea Research Part I: Oceanographic Research Papers*, 148:34–52. **https://doi.org/10.1016/j.dsr.2019.04.010**

Scientific Party, 1970. Introduction. *In* Maxwell, A.E., et al. (Eds.), *Initial Reports of the Deep Sea Drilling Project,* 3. Washington, DC (US Government Printing Office). **https://doi.org/10.2973/dsdp.proc.3.101.1970**

Shipboard Scientific Party, 1993. Explanatory notes. *In* Alt, J.C., Kinoshita, H., Stokking, L.B., et al. (Eds.), *Proceedings of the Ocean Drililng Program Initial Reports,* 148: College Station, TX (Ocean Drilling Program). **https://doi.org/10.2973/odp.proc.ir.148.101.1993**

Shipboard Scientific Party, 1997. Introduction and summary: hydrothermal circulation in the oceanic crust and its consequences on the eastern flank of the Juan de Fuca Ridge. *In* Davies, E.E., Fisher, A.T., Firth, J.V. and et al. (Eds.), *Proceedings of the Ocean Drilling Program, Initial Reports,* 168: College Station, TX (Ocean Drilling Program). 7–21. **https://doi.org/10.2973/odp.proc.ir.168.101.1997**

Shipboard Scientific Party, 2002. Leg 199 summary. *In* Lyle, M., Wilson, P.A., Janecek, T.R., et al. (Eds.), *Proceedings of the Ocean Drilling Program, Initial Reports,* 199: College Station, TX (Ocean Drilling Program). **https://doi.org/10.2973/odp.proc.ir.199.101.2002**

Shipboard Scientific Party, 2004. Leg 208 summary. *In* Zachos, J.C., Kroon, D., Blum, P., et al. (Eds.), *Proceedings of the Ocean Drilling Program, Initial Reports,* 208: College Station, TX (Ocean Drilling Program). **https://doi.org/10.2973/odp.proc.ir.208.101.2004**

Spinelli, G.A., Giambalvo, E.R., and Fisher, A.T., 2004. Sediment permeability, distribution, and influence on fluxes in oceanic basement. *In* Davis, E.E., and Elderfield, H. (Eds.), *Hydrogeology of the Oceanic Lithosphere:* Cambridge, UK (Cambridge University Press), 151–188.

Staudigel, H., Hart, S.R., Schmincke, H.-U., and Smith, B.M., 1989. Cretaceous ocean crust at DSDP Sites 417 and 418: carbon uptake from weathering versus loss by magmatic outgassing. *Geochimica et Cosmochimica Acta*, 53(11):3091–3094. **https://doi.org/10.1016/0016-7037(89)90189-0**

Stein, C.A., and Stein, S., 1994. Constraints on hydrothermal heat flux through the oceanic lithosphere from global heat flow. *Journal of Geophysical Research: Solid Earth*, 99(B2):3081–3095. **https://doi.org/10.1029/93JB02222**

Stommel, H., 1961. Thermohaline convection with two stable regimes of flow. *Tellus*, 13(2):224–230. **https://doi.org/10.1111/j.2153-3490.1961.tb00079.x**

Sylvan, J.B., Hoffman, C.L., Momper, L.M., Toner, B.M., Amend, J.P., and Edwards, K.J., 2015. *Bacillus rigiliprofundi* sp. nov., an endospore-forming, Mn-oxidizing, moderately halophilic bacterium isolated from deep subseafloor basaltic crust. *International Journal of Systematic and Evolutionary Microbiology*, 65(6):1992–1998. **https://doi.org/10.1099/ijs.0.000211**

Thomas, D.J., Bralower, T.J., and Jones, C.E., 2003. Neodymium isotopic reconstruction of late Paleocene–early Eocene thermohaline circulation. *Earth and Planetary Science Letters*, 209(3):309–322. **https://doi.org/10.1016/S0012-821X(03)00096-7**

Tobin, H.J., Kinoshita, M., Ashi, J., Lallemant, S., Kimura, G., Screaton, E.J., Thu, M.K., Masago, H., and Curewitz, D., 2008. NanTroSEIZE Stage 1 expeditions: introduction and synthesis of key results. *In* Kinoshita, M., Tobin, H., Ashi, J., Kimura, G., Lallemant, S., Screaton, E.J., Curewitz, D., Masago, H., Moe, K.T., and the Expedition 314/315/316 Scientists (Eds.), *Proceedings of the Integrated Ocean Drilling Program,* 314/315/316: Washington, DC (Integrated Ocean Drilling Program Management, Inc.). **https://doi.org/10.2204/iodp.proc.314315316.101.2009**

Tripati, A., Backman, J., Elderfield, H., and Ferretti, P., 2005. Eocene bipolar glaciation associated with global carbon cycle changes. *Nature*, 436(7049):341–346. **https://doi.org/10.1038/nature03874**

Vance, D., Teagle, D.A.H., and Foster, G.L., 2009. Variable Quaternary chemical weathering fluxes and imbalances in marine geochemical budgets. *Nature*, 458(7237):493–496. **https://doi.org/10.1038/nature07828**

Wheat, C.G., and Fisher, A.T., 2008. Massive, low-temperature hydrothermal flow from a basaltic outcrop on 23 Ma seafloor of the Cocos Plate: chemical constraints and implications. *Geochemistry, Geophysics, Geosystems*, 9(12):Q12O14. **https://doi.org/10.1029/2008GC002136**

Wilson, D.S., Teagle, D.A.H., Acton, G.D., et al., 2003. *Proceedings of the Ocean Drilling Program, Initial Reports*, 206: College Station, TX (Ocean Drilling Program). **https://doi.org/10.2973/odp.proc.ir.206.2003**

Wright, J.D., Miller, K.G., and Fairbanks, R.G., 1991. Evolution of modern deepwater circulation: evidence from the late Miocene Southern Ocean.

Paleoceanography and Paleoclimatology, 6(2):275–290. **https://doi.org/10.1029/90PA02498**

Wright, J.D., Miller, K.G., and Fairbanks, R.G., 1992. Early and Middle Miocene stable isotopes: Implications for deepwater circulation and climate. *Paleoceanography and Paleoclimatology*, 7(3):357–389. **https://doi.org/10.1029/92PA00760**

Wunsch, C., 2002. What Is the thermohaline circulation? *Science*, 298(5596):1179–1181. **https://doi.org/10.1126/science.1079329**

Zachos, J.C., Dickens, G.R., and Zeebe, R.E., 2008. An early Cenozoic perspective on greenhouse warming and carbon-cycle dynamics. *Nature*, 451(7176):279–283. **https://doi.org/10.1038/nature06588**

Zachos, J., Pagani, M., Sloan, L., Thomas, E., and Billups, K., 2001. Trends, rhythms, and aberrations in global climate 65 Ma to Present. *Science*, 292(5517):686–693. **https://doi.org/10.1126/science.1059412**

Zachos, J.C., Röhl, U., Schellenberg, S.A., Sluijs, A., Hodell, D.A., Kelly, D.C., Thomas, E., et al., 2005. Rapid acidification of the ocean during the Paleocene-Eocene Thermal Maximum. *Science*, 308(5728):1611–1615. **https://doi.org/10.1126/science.1109004**

Zeebe, R.E., Zachos, J.C., Caldeira, K., and Tyrrell, T., 2008. Oceans: carbon emissions and acidification. *Science*, 321(5885):51–52. **https://doi.org/10.1126/science.1159124**

Table T1. Site background information updated based on Expedition 390C findings. NA = not applicable; sites were not visited during Expedition 390C.

Site	Hole	Age (Ma)	Half-spreading rate (mm/y)	Estimated sediment thickness (mbsf)	Observed sediment thickness (mbsf)	Average sediment accumulation rate (m/My)	Total penetration (m)
U1556	A	61.2	13.5	180	278.0	4.54	283.8
U1557	B	61.2	13.5	510.0	564.0	9.22	574.0
U1558	A	49.2	19.5	148	158.9	3.23	163.9
SATL-33B	NA	30.6	24.0	138	NA	4.51	NA
SATL-25A	NA	15.2	25.5	104	NA	6.84	NA
U1559	A	6.6	17.0	50	64.0	9.70	66.2

Table T2. Expedition 390C site summary. APC = advanced piston corer, XCB = extended core barrel, UTC = Universal Time Coordinated.

Hole	Latitude	Longitude	Water depth (m)	Total penetration (m)	Drilled interval (m)	Cored interval (m)	Core recovered (m)	Recovery (%)	Total cores (*N*)	APC cores (*N*)	XCB cores (*N*)	Start date	Start time UTC (h)	End date	End time UTC (h)	Time on hole (h)	Time on hole (days)
U1556A	30°56.5244′S	26°41.9472′W	5006.37	283.8	NA	283.3	243.78	86	33	16	17	28 Oct 2020	0130	1 Nov 2020	0310	97.68	4.07
		Site U1556 totals:		283.8	NA	283.3	243.78		33	16	17					97.68	4.07
U1557A	30°56.4549′S	26°37.7912′W	5012.28	9.5	NA	9.5	9.63	101	1	1	0	1Nov 2020	0740	1 Nov 2020	1345	6.00	0.25
U1557B	30°56.4547′S	26°37.7775′W	5012.28	574.0	NA	574.0	414.94	72	66	11	55	1 Nov 2020	1345	9 Nov 2020	0110	179.52	7.48
U1557C	30°56.4646′S	26°37.7897′W	5012.28	3.0	3.0	NA	NA	NA	NA	NA	NA	9 Nov 2020	0110	9 Nov 2020	1835	17.52	0.73
U1557D	30°56.4651′S	26°37.7892′W	5010.66	64.2	64.2	NA	NA	NA	NA	NA	NA	9 Nov 2020	1835	12 Nov 2020	0808	61.44	2.56
		Site U1557 totals:		650.7	67.2	583.5	424.57		67	12	55					264.48	11.02
U1558A	30°53.7728′S	24°50.4970′W	4336.87	163.9	NA	163.9	138.69	85	19	11	8	12 Nov 2020	1630	15 Nov 2020	0610	61.68	2.57
U1558B	30°53.7707′S	24°50.4843′W	4336.81	161.1	161.1	NA	NA	NA	NA	NA	NA	15 Nov 2020	0610	18 Nov 2020	1900	84.72	3.53
U1558C	30°53.7761′S	24°50.4942′W	4336.86	162.7	162.7	NA	NA	NA	NA	NA	NA	18 Nov 2020	1900	21 Nov 2020	0956	62.88	2.62
U1558D	30°53.7814′S	24°50.4822′W	4334.44	150.0	150.0	NA	NA	NA	NA	NA	NA	21 Nov 2020	0956	23 Nov 2020	2256	60.96	2.54
		Site U1558 totals:		637.7	473.8	163.9	138.69		19	11	8					270.24	11.26
U1559A	30°15.6335′S	15°2.0942′W	3055.72	66.2	NA	66.2	58.01	88	9	4	5	25 Nov 2020	1640	26 Nov 2020	2120	28.56	1.19
U1559B	30°15.6336′S	15°2.0941′W	3055.04	58.9	58.9	NA	NA	NA	NA	NA	NA	26 Nov 2020	2120	28 Nov 2020	1715	43.92	1.83
		Site U1559 totals:		125.1	58.9	66.2	58.01		9	4	5					72.48	3.02
		Expedition totals:		1697.3	599.9	1096.9	865.05		128	43	85					704.88	29.37

Table T3. Summary of outreach posts on social media and audience engagement.

Platform	Posts (*N*)	Analytics	Notes
Facebook	95	12879 engagements (comments, shares, likes, or clicks on parts of the post)	
Twitter	137	14889 engagements (including 639 retweets, 99 comments, 3731 likes), 74 new followers	Does not include retweets of other accounts.

Figure F1. Overview of the South Atlantic Transect (SAT) study region. Top: bathymetry (Ryan et al., 2009). Bottom: magnetic anomalies (Maus et al., 2009). Inset shows regional setting. Black lines = Crustal Reflectivity Experiment Southern Transect (CREST) seismic reflection profiles. Expeditions 390C, 390, and 393 sites are displayed with black (primary) and gray (alternate) dots. White circles = DSDP Leg 3 sites. WOCE = World Ocean Circulation Experiment.

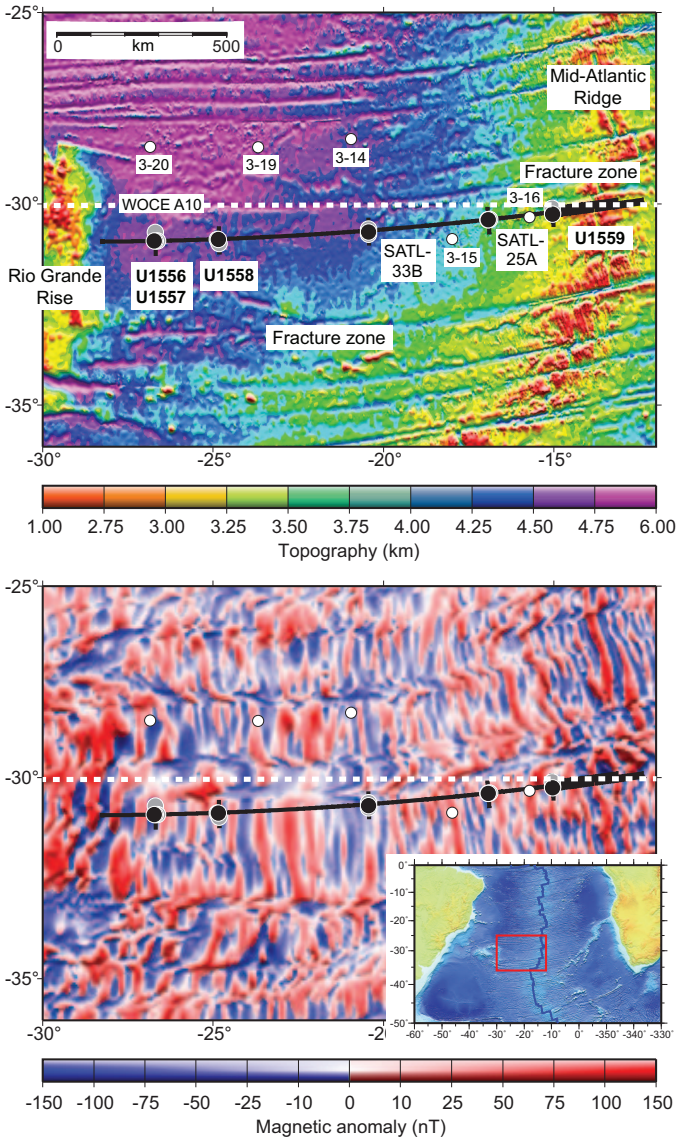

Figure F2. A. Schematic architecture of a mid-ocean ridge flank (not to scale) that illustrates parameters that may influence the intensity and style of hydrothermal alteration and the hypothetical trajectory of the 120°C isotherm with crustal age. Arrows indicate heat (red) and fluid (blue) flow. B. Calculated global hydrothermal heat flow anomaly, which decreases to 0 by 65 Ma on average, and hypothetical variations in fluid flow and chemical exchange and crustal properties that could be measured to investigate the intensity and style of ridge flank hydrothermal circulation (e.g., porosity, permeability, and two possible scenarios for alteration intensity). (After Coggon and Teagle, 2011; Expedition 335 Scientists, 2012; and an original figure by K. Nakamura, AIST.)

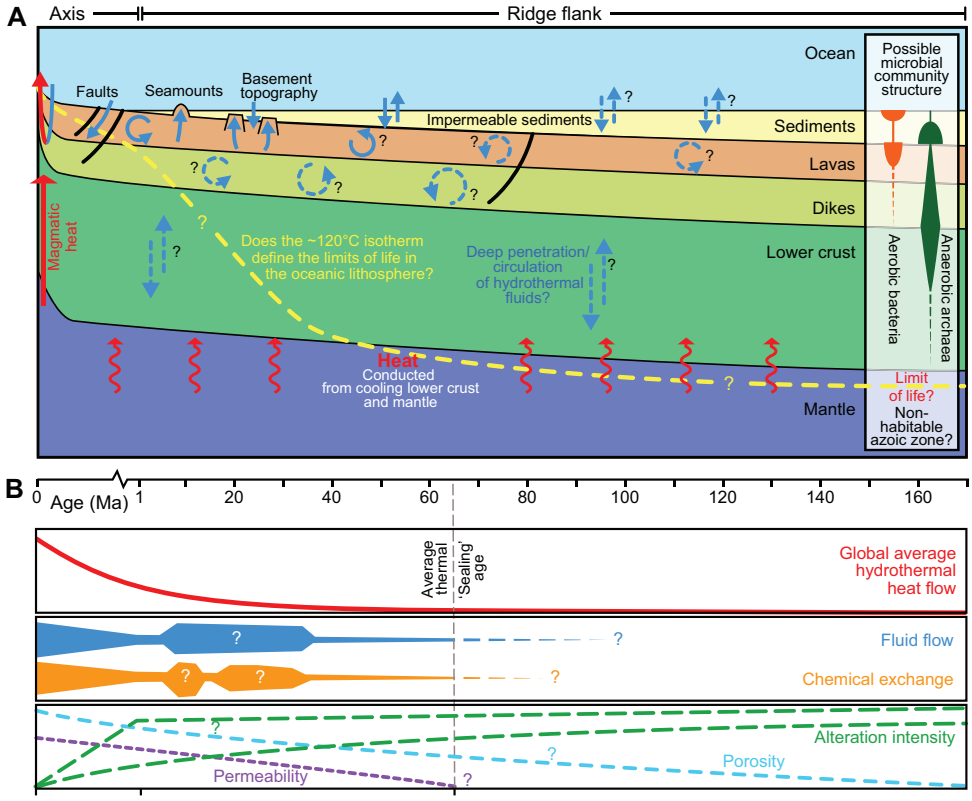

Figure F3. Sediment cover versus crustal age for Expeditions 390C, 390, and 393 primary (yellow) and alternate (orange) sites. The sediment thicknesses at all DSDP/ODP/Integrated Ocean Drilling Program/IODP drill holes that cored more than 100 m into basement of intact oceanic crust and tectonically exposed lower crust/upper mantle are shown for comparison (blue diamonds). Red line = global average sediment thickness versus age (red dashed line = ± 1σ variation) (after Spinelli et al., 2004).

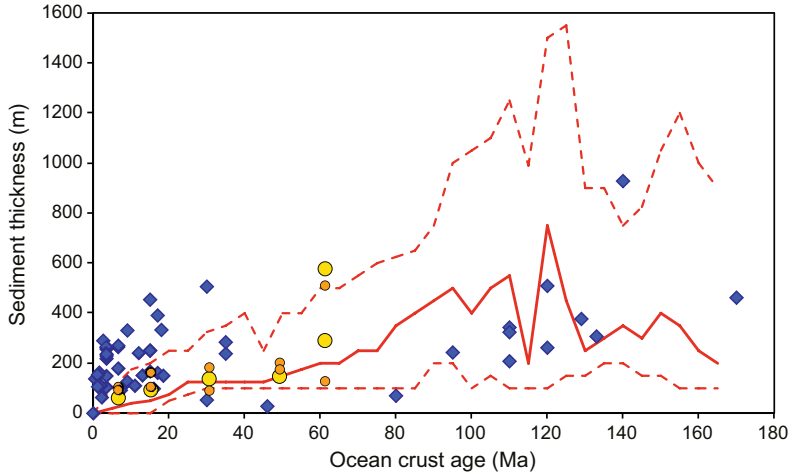

Figure F4. Seismic reflection profiles for Expedition 390C sites. Black lines = cored depth. TWT = two-way traveltime, CDP = common depth point.

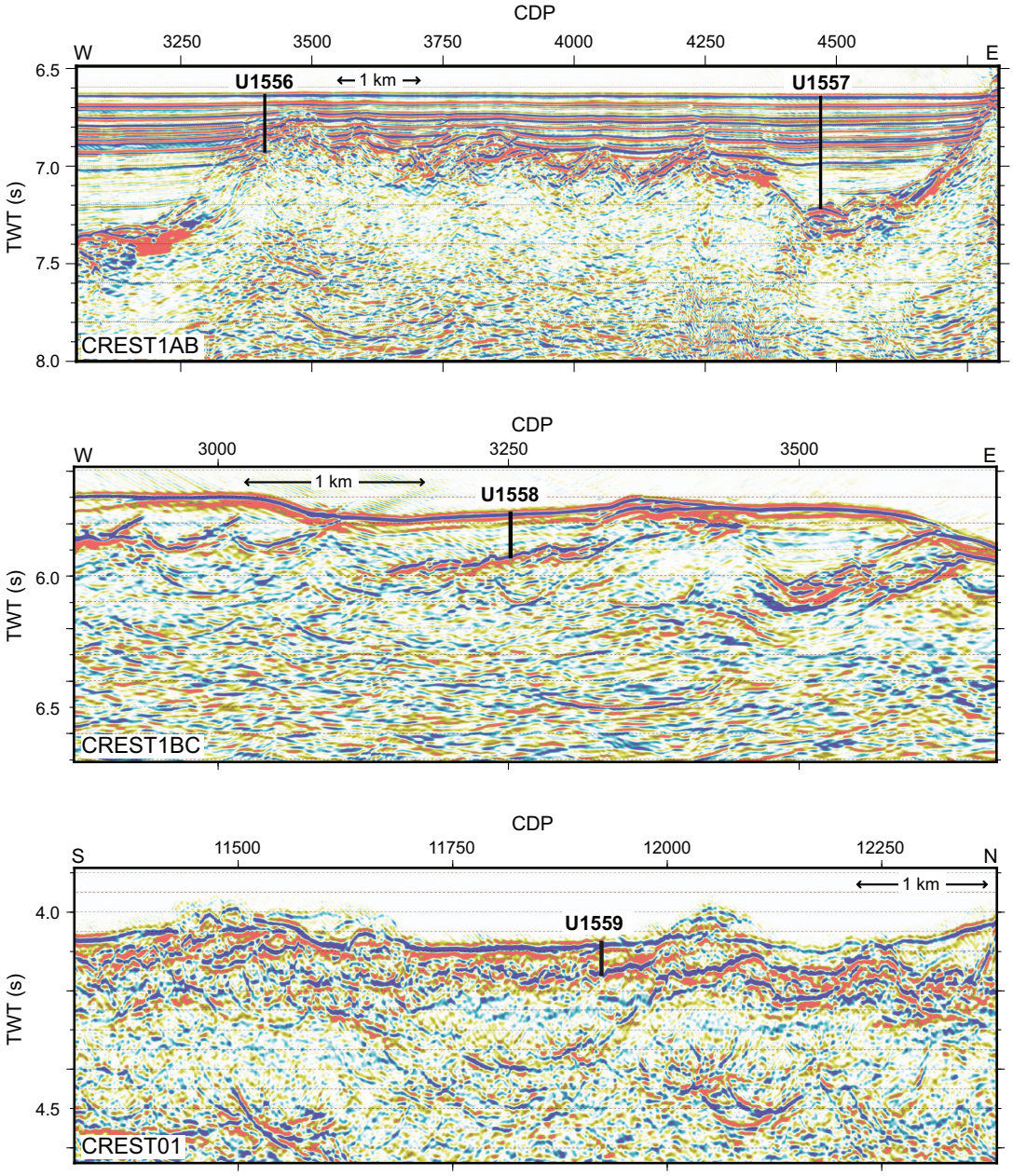

Figure F5. Compilation of all scientific ocean drilling holes that penetrate >100 m into intact upper (basaltic) ocean crust versus crustal age.

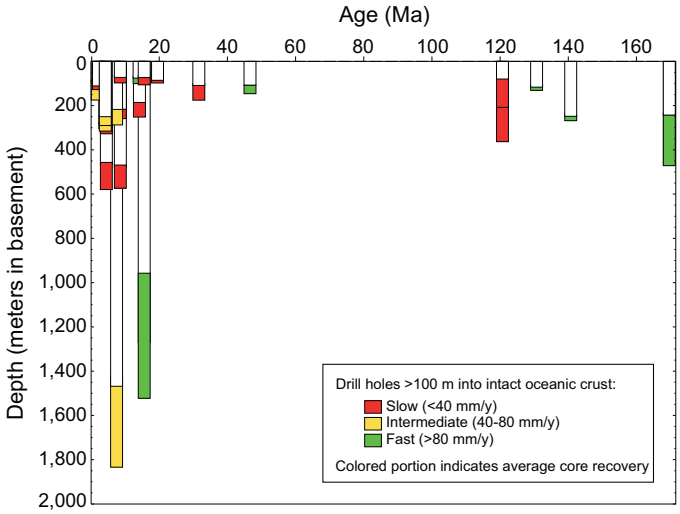

Figure F6. Pictures of cored hard rock material from each site.

Figure F7. Core recovery plots, Holes U1556A, U1557B, U1558A, and U1559A. Black = recovered core, white= no recovery.

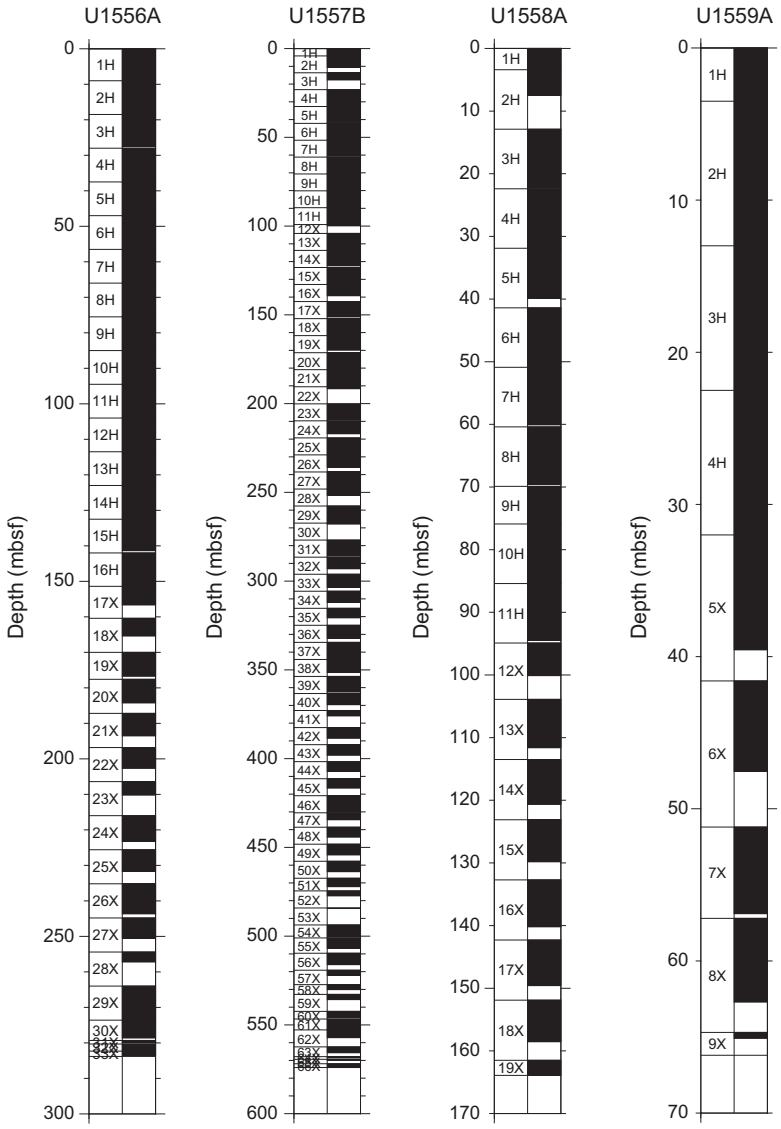

Figure F8. Reentry system, casing, and bottom-hole assembly, Hole U1557D. RCB = rotary core barrel.

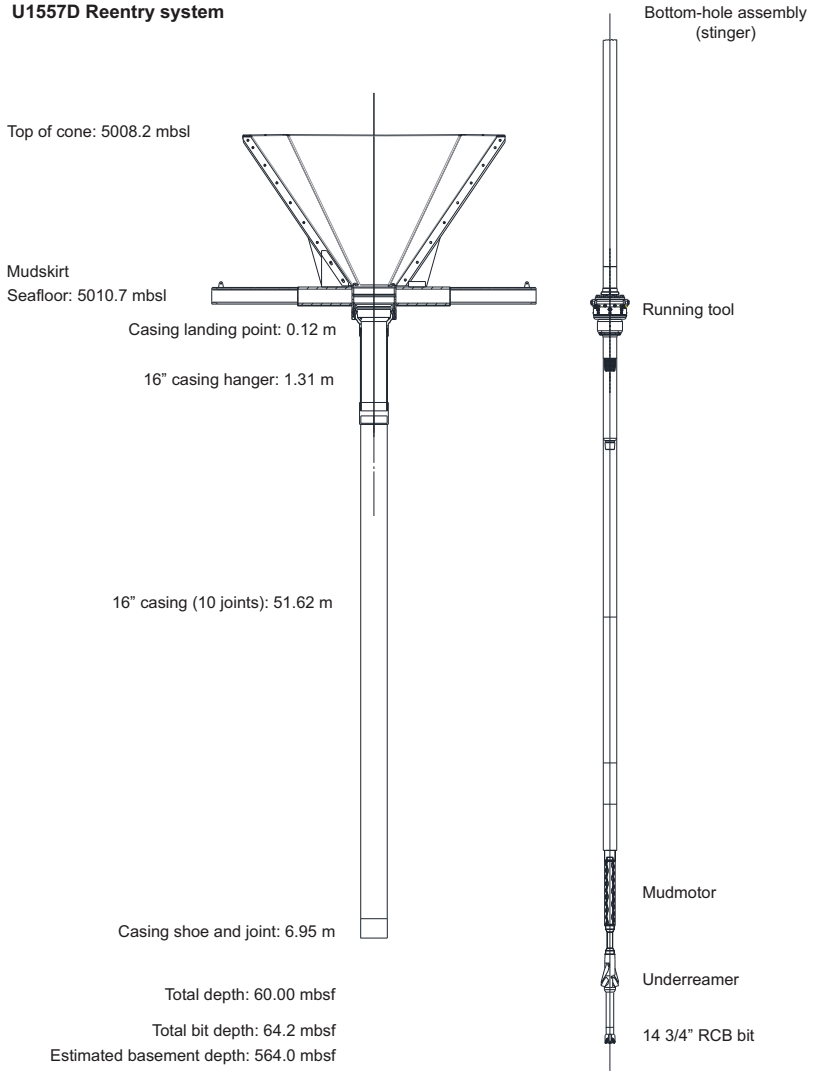

Figure F9. Reentry system, casing, and bottom-hole assembly, Hole U1558D. RCB = rotary core barrel.

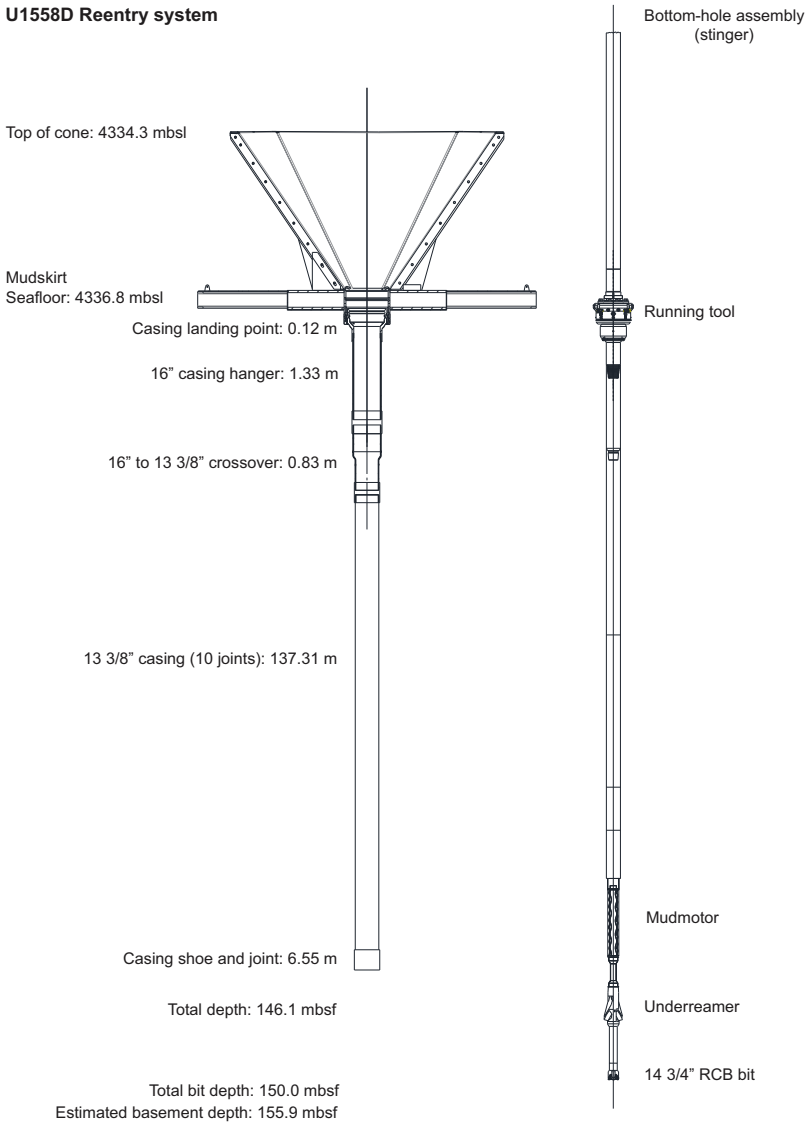

Figure F10. Hole locations, Site U1558. Top: geographic coordinates of the ship position (averaged over several hours) shown in black and gray. Red circles show approximate positions on the seafloor, relative to the westernmost hole (U1558C). Bottom: stills of video footage recorded during the search for the U1558D reentry cone showing the seafloor locations of holes. The lower image is flipped so that both images are oriented with north up. Rotation of the mudskirt on the seafloor during attempted disconnects caused the target patterns visible around Holes U1558B and U1558C and provides a scale for the images. The edge of the U1558D reentry cone is just visible behind the casing.

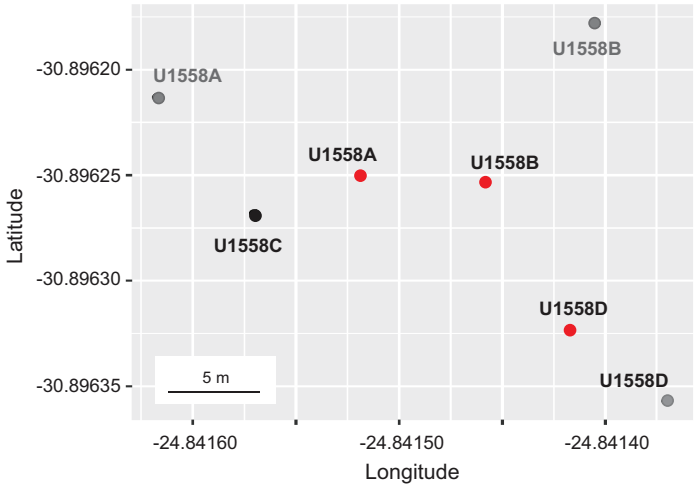

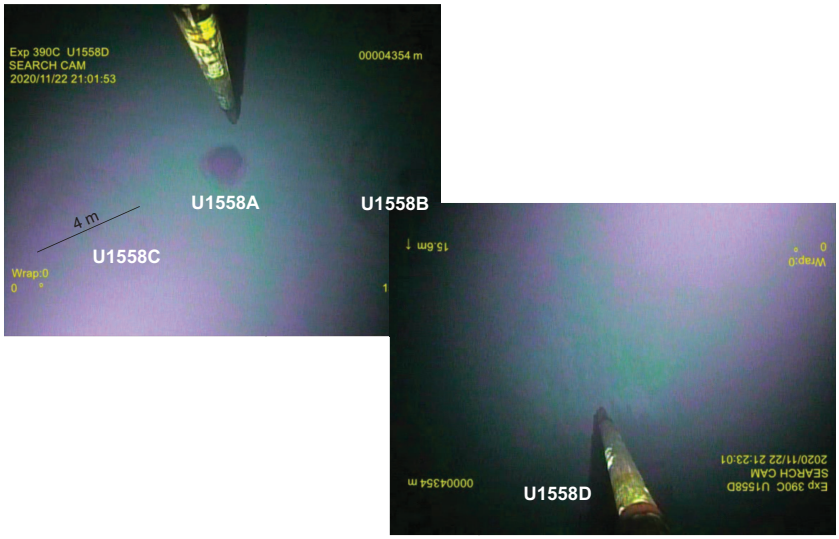

Figure F11. Reentry system, casing, and bottom-hole assembly, Hole U1559B. RCB = rotary core barrel.

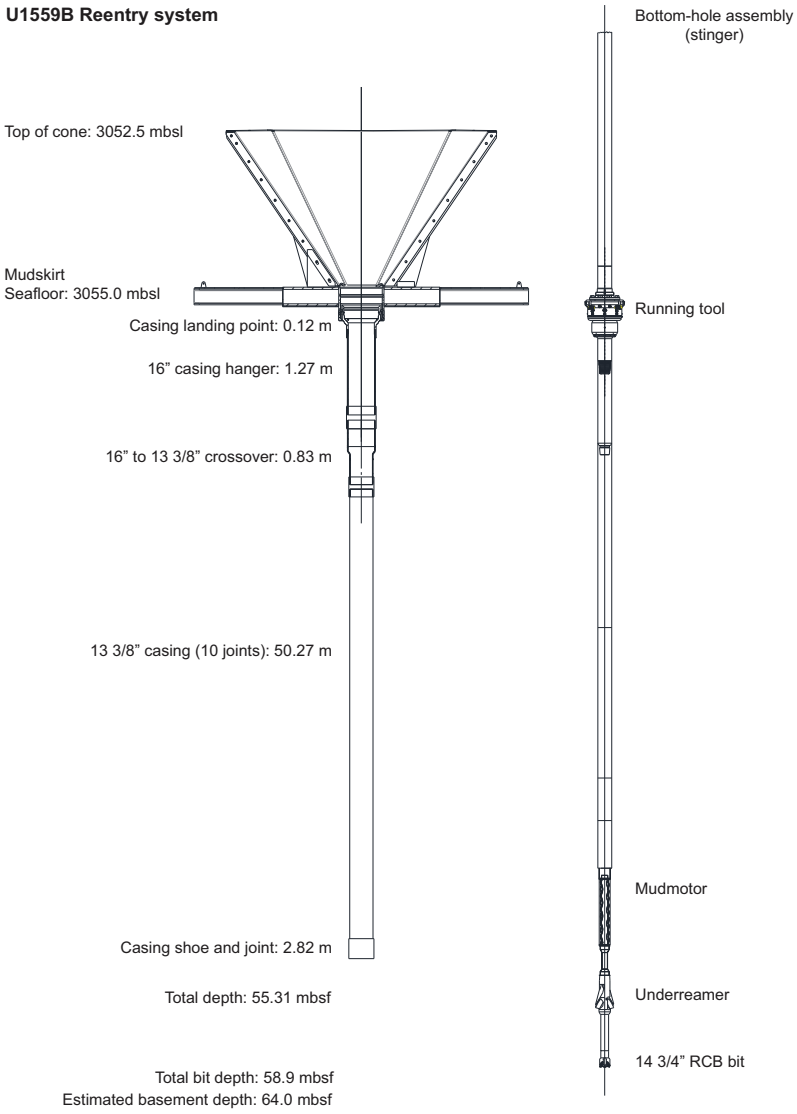

Figure F12. Transit and site location map, Expedition 390C.

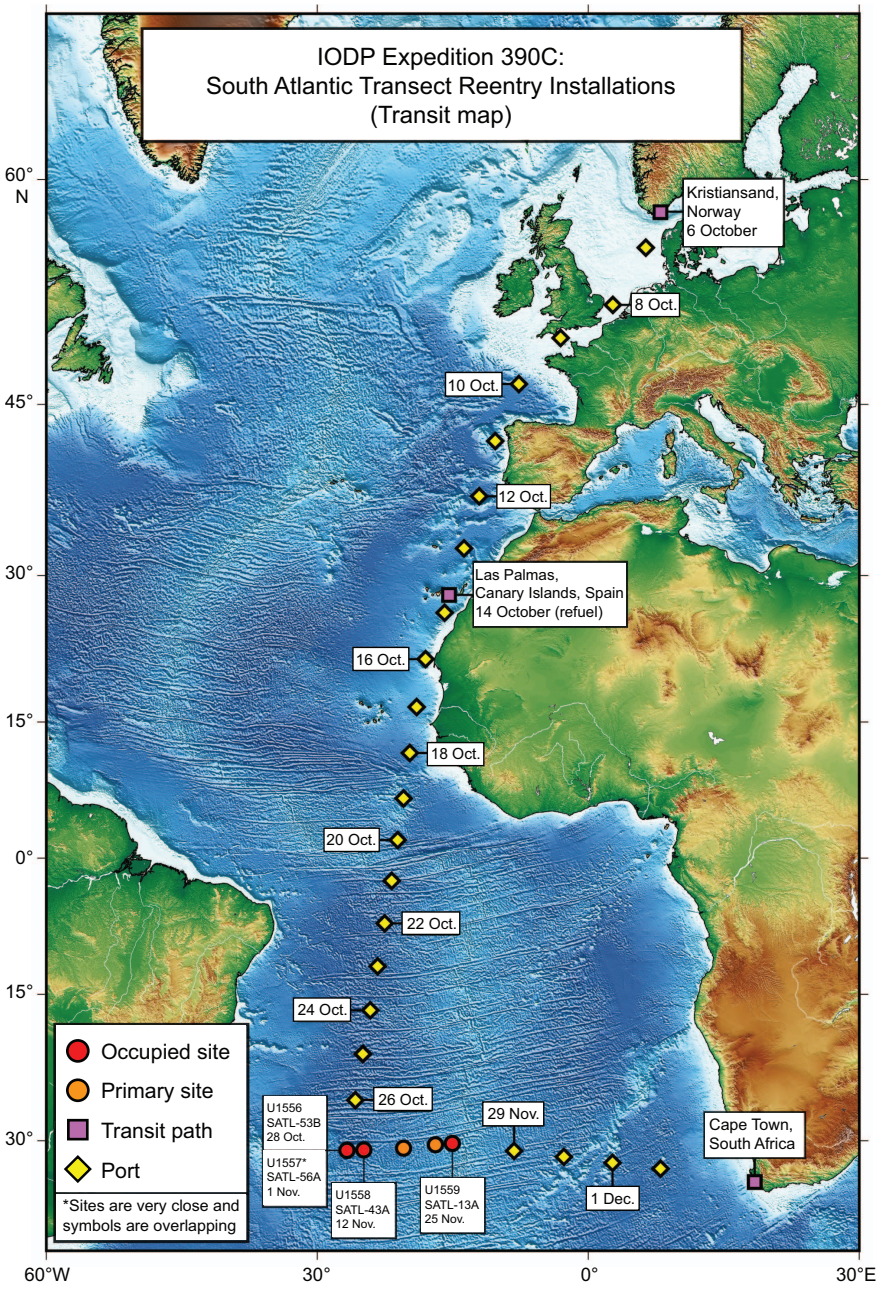

Figure F13. Operations schedule, Expedition 390C. WOW = waiting on weather.

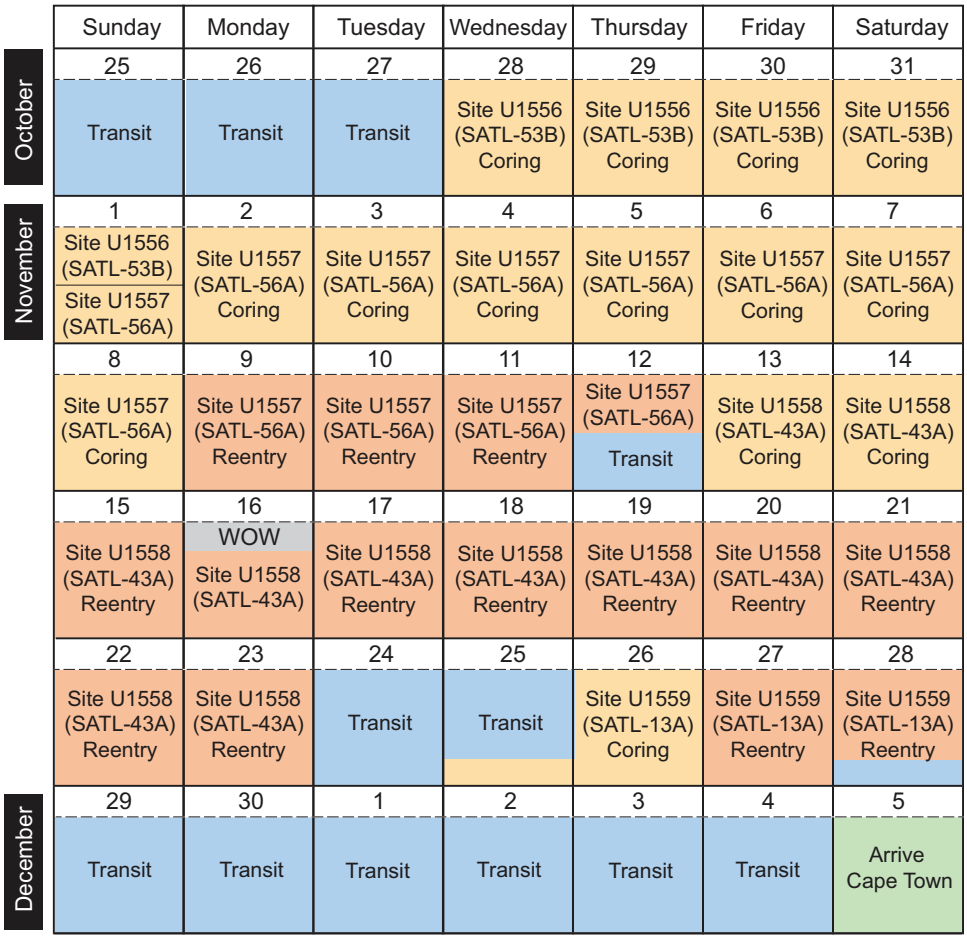

Figure F14. Accomplished operations and remaining work to be done at South Atlantic Transect sites.